University of Illinois at Urbana-Champaign

Air Conditioning and Refrigeration Center A National Science Foundation/University Cooperative Research Center

A Study of the Application of Vortex Generators to Enhance the Air-Side Performance of Heat Exchangers

B. R. Bull and A. M. Jacobi

ACRC TR-214 May 2003

For additional information:

Air Conditioning and Refrigeration Center
University of Illinois
Mechanical & Industrial Engineering Dept.
1206 West Green Street
Urbana, IL 61801

(217) 333-3115

Prepared as part of ACRC Project #121
A Study of the Application of Vortex Generators to Enhance the Air-Side Thermal Performance of Heat Exchangers
A. M. Jacobi, Principal Investigator

The Air Conditioning and Refrigeration Center was founded in 1988 with a grant from the estate of Richard W. Kritzer, the founder of Peerless of America Inc. A State of Illinois Technology Challenge Grant helped build the laboratory facilities. The ACRC receives continuing support from the Richard W. Kritzer Endowment and the National Science Foundation. The following organizations have also become sponsors of the Center.

Alcan Aluminum Corporation
Amana Refrigeration, Inc.
Arçelik A. S.
Brazeway, Inc.
Carrier Corporation
Copeland Corporation
Dacor
Daikin Industries, Ltd.
Delphi Harrison Thermal Systems
Embraco S. A.
General Motors Corporation
Hill PHOENIX
Honeywell, Inc.
Hydro Aluminum Adrian, Inc.
Ingersoll-Rand Company
Kelon Electrical Holdings Co., Ltd.
Lennox International, Inc.
LG Electronics, Inc.
Modine Manufacturing Co.
Parker Hannifin Corporation
Peerless of America, Inc.
Samsung Electronics Co., Ltd.
Sanyo Electric Co., Ltd.
Tecumseh Products Company
The Trane Company
Valeo, Inc.
Visteon Automotive Systems
Wieland-Werke, AG
Wolverine Tube, Inc.

For additional information:

Air Conditioning & Refrigeration Center
Mechanical & Industrial Engineering Dept.
University of Illinois
1206 West Green Street
Urbana, IL 61801

217 333 3115

Abstract

The effect of longitudinal vortex generation on heat transfer is evaluated for a full scale plain fin-and-tube compact heat exchanger operating in both dry and wet conditions. The heat exchanger tested is comparable to an evaporator in a residential air-conditioning system. For this study the baseline performance of the heat exchanger is determined then the heat exchanger is modified with the addition of 2100 delta-wing vortex generators.

The performance is determined by a volume goodness factor for the dry operating conditions and the overall enthalpy transfer coefficient for wet operating conditions. A 10% improvement in the volume goodness factor was recorded for the dry tests and the wet tests showed an overall reduction in the overall enthalpy transfer coefficient. A comparison was then made using j and f correlations for other enhanced surfaces. From these tests the j/f value for the vortex generator enhanced surface is shown to be comparable to the other enhanced surfaces.

Table of Contents

Page

Abstract iii

List of Figures v

List of Tables vi

Nomenclature vii

Chapter 1. Introduction 1

1.1 Motivation 1

1.2 Literature Review 2

1.3 Project Objectives 3

Chapter 2. Experimental Apparatus 4

2.1 Wind Tunnel 4

2.2 Test Specimen 5

Chapter 3. Procedure 7

Chapter 4. Results 9

4.1 Data Reduction 9

4.2 Analysis 12

Chapter 5. Comparison 16

Chapter 6. Summary and Conclusions 21

References 22

Appendix A 23

A.1 Energy Balance 23

A.2 Testing Conditions 23

A.3 Weighted Least-Squares Reduction 24

A.4 Surface Efficiency 24

A.5 Input Values 27

Appendix B. EES Code 30

List of Figures

Page

Figure 1.1.1 A delta-wing vortex generator where b = base length, c = chord length, and a = angle of attack. 1
Figure 1.1.2 Several types of vortex generators: 1. delta wing, 2. rectangular wing, 3. delta winglet, 4. rectangular winglet. Adapted from [10]. 2
Figure 2.1.1 Schematic of closed loop wind tunnel used for testing: 1. Flow nozzle, 2. Hygrometer taps, 3. Mixing chamber, 4. Test Section, 5. Steam injection, 6. Blower, 7. Resistance heaters. 4
Figure 2.1.2 Enlarged view of test section: 1. Downstream pressure taps, 2. Upstream pressure taps, 3. Upstream thermopiles, 4. Heat exchanger, 5. Condensate collector, 6. Downstream thermopiles. 5
Figure 2.2.1 Cross-section of heat exchanger from side (A) and top (B) with vortex generators attached. Dimensions: F_P = 1.7 mm, F_t = 0.102 mm, P_L = 24 mm, P_T = 25 mm, f = 10 mm, g = 7 mm, h = 9 mm. 6
Figure 3.1 Energy balance for all tests performed. 8
Figure 4.1.1 Resistance network for a heat exchanger. 10
Figure 4.2.1 Air-side thermal resistance from Wilson plot technique for dry tests. 13
Figure 4.2.2 Air-side thermal resistance from Wilson plot technique for wet tests. 13
Figure 4.2.3 Air-side pressure drop across the heat exchanger for dry tests. 14
Figure 4.2.4 Air-side pressure drop across the heat exchanger for wet tests. 14
Figure 4.2.5 Dry volume goodness data for baseline and enhanced tests. 15
Figure 4.2.6 Wet overall heat transfer coefficient for baseline and enhanced tests. 15
Figure 5.1 Colburn j factors for vortex generator and other enhanced surfaces for dry conditions. 18
Figure 5.2 Friction factors for vortex generator and other enhanced surfaces for dry conditions. 18
Figure 5.3 j/f for vortex generator and other enhanced surfaces for dry conditions. 19
Figure 5.4 Colburn j factors for vortex generator and other enhanced surfaces for wet conditions. 19
Figure 5.5 Friction factors for vortex generator and other enhanced surfaces for wet conditions. 20
Figure 5.6 j/f for vortex generator and other enhanced surfaces for wet conditions. 20
Figure A.3.1 Wilson Plot sets with WLSE fit extrapolated. 25
Figure A.3.2 Schematic of sector method used to calculate fin efficiency. 25

List of Tables

Page

Table A.2 Environmental operating conditions. 23
Table A.5.1 A list of all input test values.....27

Nomenclature

a	Angle of attack [°]
A_{ff}	Minimum free flow area [m^2]
A_f	Tube surface area [m^2]
A_{fr}	Frontal area [m^2]
A_t	Total heat transfer surface area [m^2]
b	Base length of vortex generator [mm]
c	Chord length of vortex generator [mm]
cp	Specific heat [J/kg-K]
D_C	Fin collar diameter [mm]
D_H	Hydraulic diameter [m]
D_M	Tube major diameter (for a flat tube) [mm]
D_O	Outer diameter (for a round tube) [mm]
E	Fan power per unit core volume [kW/m^3]
f	Friction factor
F	Cross-flow correction factor
F_D	Flow depth [mm]
F_P	Fin pitch [mm]
F_L	Fin length [mm]
F_t	Fin thickness [mm]
h	Convective heat transfer coefficient [W/m^2-K]
I	Enthalpy [kJ/kg]
j	Colburn j-factor
k	Thermal conductivity [W/m-K]
L	$P_L/2$ [mm]
L_L	Louver length [mm]
L_P	Louver pitch [mm]
M	$P_T/2$ [mm]
$\dot{m}$	Mass flow rate [kg/s]
N	Number of tube passes or total number of sectors in a zone
Nu	Nusselt number
P	Pressure [Pa]
P_L	Longitudinal tube pitch [mm]
P_T	Transverse tube pitch [mm]
Pr	Pandtl number
Q	Heat transfer rate [W]
R	Resistance [K/W] or radius ratio R_o/R_i
r	Radius [m]
Re	Reynolds number
S	Surface area [m^2]
St	Stanton number
T	Temperature [°C]
T_D	Tube depth (flat tube) [mm]
T_P	Tube pitch [mm]
U	Heat transfer conductance [W/m^2-K]

V	Velocity [m/s]
Z	Heat transfer per unit T per unit core volume [kW/K-m^3]

GREEK SYMBOLS

ß	Heat transfer surface area per unit core volume [m^2/m^3]
d_F	Fin thickness [mm]
$?_O$	Surface efficiency
$?_f$	Fin efficiency
n	Kinematic viscosity [m^2/s]
µ	Viscosity [kg/s-m]
?	Density [kg/m^3]
s	Uncertainty
?	Louver angle [°]

SUBSCRIPTS

A	Air-side
AVG	Average
D	Diameter
DH	Hydraulic diameter
ds	downstream
f	fin
i	Inner
LM	Log-mean
lp	Louver pitch
o	Outer
R	Refrigerant-side
t	Total
us	Upstream
w	Water

Chapter 1. Introduction

1.1 Motivation

Air-side thermal resistance is an important factor in designing a compact heat exchanger. In fact, the purpose of a compact heat exchanger is to present a large heat transfer surface area to compensate for the poor convection coefficient of air. Enhancement of a heat transfer surface will improve the performance of the heat exchanger and can thus reduce its volume, its material cost, and maybe its operating cost. Traditional methods of reducing the air-side thermal resistance have involved increasing the surface area of the heat exchanger, increasing the length of air pathlines, or reducing the thermal boundary layer thickness on the heat exchanger surface. Increasing the surface area is effective but results in an increased material cost and an increased mass for the heat exchanger. Increasing pathlines is primarily accomplished by redirecting the flow as with a louvered-fin array. Current industry methods to reduce thermal boundary layer thickness primarily involve restarting the boundary layer. An example of this technique is the use of an offset strip fin array.

Another possible method to reduce boundary layer thickness is by passive vortex generation. In this technique the flow field is altered by an obstruction to generate a vortex oriented in the direction of the flow. Such a streamwise vortex creates what have been referred to as downwash and upwash regions [1]. Figure 1.1.1 shows the vortices created by a delta-wing vortex generator. Figure 1.1.2 shows various types of vortex generator geometries. The resulting change in the flow alters the local thermal boundary layer. The net effect of this manipulation is an average increase in heat transfer for the affected area. Previous research has been conducted to evaluate the performance of vortex generators in various environments. The results of this research show promising results for the full-scale application of vortex generators.

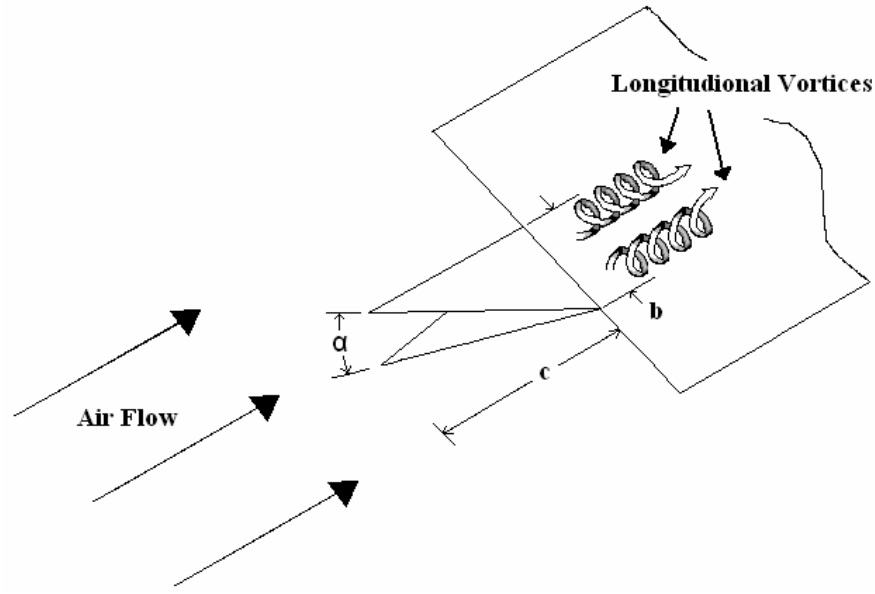

Figure 1.1.1 A delta-wing vortex generator where b = base length, c = chord length, and a = angle of attack.

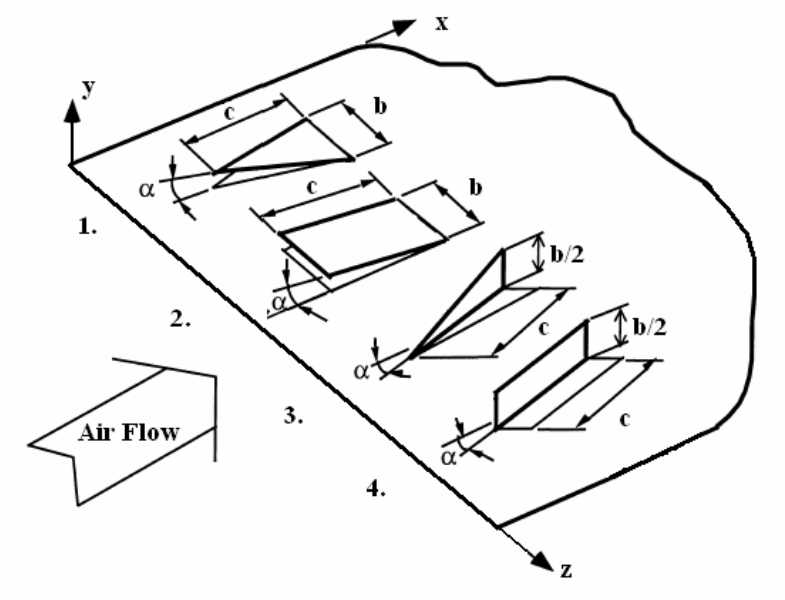

Figure 1.1.2 Several types of vortex generators: 1. delta wing, 2. rectangular wing, 3. delta winglet, 4. rectangular winglet. Adapted from [10].

1.2 Literature Review

Extensive reviews of the early study of interactions between vortices and boundary layers exist in the literature [1,2,3]. A survey of relevant work conducted since these reviews were published will be presented.

Torii *et al.* [4,5] conducted multiple experiments to determine the heat transfer enhancement of delta-winglet vortex generators. Hot-wire anemometry, naphthalene sublimation, smoke-wire flow visualization, constant heat flux, and a modified single-blow technique have been used to characterize the performance of the vortex generators. From the naphthalene sublimation tests [4] a local heat transfer enhancement of 200% was reported in the downwash region of the vortex. A more recent experiment [5] has been performed to study the effect of delta-winglet vortex generators on a heat exchanger element with various finned-tube bundle arrangements. A modified single-blow method was used to evaluate the performance of various configurations of tubes and delta-winglet vortex generators. The resulting enhancement for the addition of vortex generators to a three row in-line tube bundle arrangement was a 10-25% heat transfer enhancement and a 20-35% increase in pressure drop for a Reynolds number range of 300-2700. The characteristic length for the Reynolds number is twice the channel height.

For over ten years Fiebig *et al.* [2,3,6-8] have been studying vortex generators both numerically and analytically. In 1993, Fiebig [6] tested a fin-and-tube heat exchanger element with a pair of delta-winglet vortex generators downstream of each tube. They found that the vortex generators increased the heat transfer by 55-65%, with a corresponding increase of 20-45% in the friction factor. Their conclusion was that “results indicate that the vortex generators have the potential to reduce considerably the size and mass of heat exchangers for a given heat load.” Fiebig [7] also performed a performance evaluation comparison between vortex generator enhancement and other enhancement techniques. These other surfaces included an offset strip fin array, a louvered fin array, and a plain fin-and-tube heat exchanger. In this study thermal-hydraulic performance for the surface with vortex generators was obtained from a numerical simulation, and the results for the other surfaces were obtained from

published experimental data. In comparing a plain fin with a rectangular cross section to a vortex generator enhanced surface, their results showed that the vortex generator provided the best performance with a 76% reduction in the heat transfer surface area for a fixed heat duty and pumping power. In a more recent study, Fiebig [8] in 2000 studied the enhancement from staggered punched vortex generators on a finned oval tube heat exchanger element. A finite volume technique was used to study "hydrodynamically and thermally developing laminar flow (Re equals 300) and conjugate heat transfer." The results were presented in the form of the ratio of the Area Goodness Factors $(j/j_0)/(f/f_0)$. For two staggered winglets an enhancement of 15.1% was measured and for four staggered winglets the enhancement was 9.1%.

Gentry [9] used flow visualization and naphthalene sublimation techniques to determine the heat transfer enhancement available from vortex generators in plate and channel flows. The local and average heat transfer enhancement was determined using the heat and mass transfer analogy. For flat plate flow a maximum local enhancement of 300% was measured and average enhancements of 35%, 60%, and 80% were measured for Re_C = 300, 800, and 1300, respectively. For these measurements the Reynolds number was based on the channel height.

ElSherbini [10] tested delta-wing vortex generators on a plain-fin-and-tube heat exchanger. These tests were performed on a heat exchanger used as a refrigeration evaporator. The performance enhancement was evaluated by the Area Goodness Factor. A j/f enhancement of 29-34% was measured over the Reynolds number range tested. A maximum air-side heat transfer enhancement of 31.3% over the baseline performance was observed. The pressure drop penalty associated with this enhancement was less than 10%.

1.3 Project Objectives

A substantial amount of research has been performed to determine the potential use of vortex generators for heat transfer enhancement. In this prior research vortex structure, strength, trajectory, the local heat transfer enhancement, and pressure drop penalties have been studied. Much less work has been reported on vortex-generator implementation on production heat exchangers, which have numerous challenges due to fin geometry and operating conditions. Moreover, to the author's knowledge their have been no studies of vortex generator enhancement under wet surface conditions published in the open literature.

This thesis focuses on the application of vortex generators to a full scale plain fin-and-tube compact heat exchanger. The heat exchanger tested is comparable to an evaporator in a residential air-conditioning system. The concerns encountered in full scale testing are geometric and environmental. In the developing channel flows previously tested, the effect of the refrigerant tube is neglected. The environmental concern is manifested in the fact that condensation formation on an evaporator in an air-conditioning system is unavoidable in normal operation. This research evaluates the performance enhancement of delta-wing vortex generators in normal operating ranges for a residential air-conditioning evaporator. The resulting benefit is then compared to other enhancement techniques.

Chapter 2. Experimental Apparatus

2.1 Wind Tunnel

The heat transfer experiments were conducted in the closed-loop wind tunnel shown in Figures 2.1.1 and 2.1.2. The wind tunnel is primarily constructed of Plexiglas and steel. Downstream from the test specimen, the air passes through a blower motor which controls the upstream air velocity in the wind tunnel. The air then passes through a steam injection area, where the humidity level of the air is controlled. Proportional-Integral-Derivative (PID) controlled resistance heaters are used to modulate the air temperature for desired testing conditions. The air then passes through a nozzle to measure the mass flow rate of air, which in turn is used to determine the face velocity at the heat exchanger. The conditioned air then passes through a mixing chamber with flow straighteners to increase the uniformity of the flow. Finally, the air enters a contraction which leads to the test section.

The test section of the wind tunnel can be separated into three components: upstream, specimen, and downstream. The upstream section has six thermopiles to measure the upstream temperature and four pressure taps that are connected to a pressure transducer. A hygrometer is attached to the mixing chamber to determine the dew point temperature of the upstream air. The test specimen is positioned on a trough which collects the condensate that drains from the heat exchanger. The heat exchanger is surrounded by Plexiglas which connects to the duct upstream and downstream to ensure no leakage or infiltration in the loop. Flow contractors are located immediately upstream, and flow expanders downstream, to adjust the cross-sectional area of the wind tunnel so that it matches the area of the heat exchanger. The downstream area has twelve thermopiles to measure the downstream temperature, a hygrometer to measure the downstream dew point temperature, and four pressure taps that are also connected to the pressure transducer. The pressure transducer then measures the pressure difference across the heat exchanger.

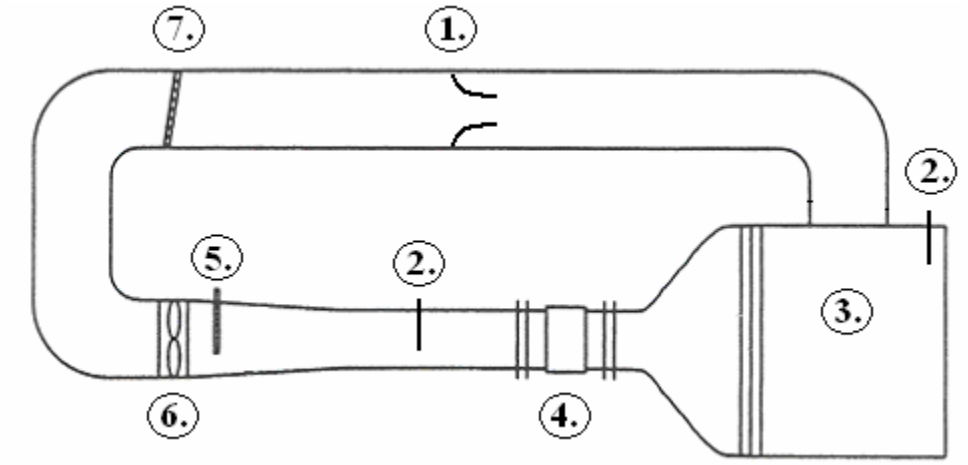

Figure 2.1.1 Schematic of closed loop wind tunnel used for testing: 1. Flow nozzle, 2. Hygrometer taps, 3. Mixing chamber, 4. Test Section, 5. Steam injection, 6. Blower, 7. Resistance heaters.

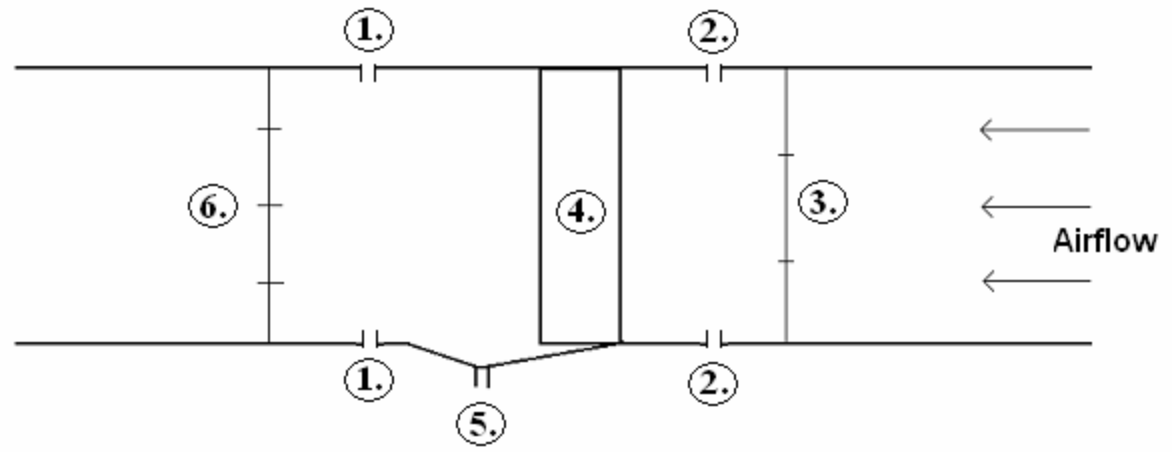

Figure 2.1.2 Enlarged view of test section: 1. Downstream pressure taps, 2. Upstream pressure taps, 3. Upstream thermopiles, 4. Heat exchanger, 5. Condensate collector, 6. Downstream thermopiles.

The refrigerant side of the heat exchanger is connected to a chiller system to provide a constant temperature inlet condition. An ethylene glycol based coolant, DOWTHERM 4000, is diluted with water to a mass concentration of 40% and used as the coolant. Resistive Thermal Devices (RTDs) are placed in the inlet and exit lines attached to the heat exchanger. Mixing cups are placed upstream of these RTDs to ensure an appropriate average coolant temperature reading. The coolant properties are obtained from data provided by the manufacturer.

All data are obtained using a data acquisition system monitored by a Labview program. The data acquisition system consists of a National Instruments SCXI-1102 Signal Conditioning Module, a SCXI-1303 Terminal Block, and a SCXI-1000 Signal Conditioning Chassis, which is connected to a PCI-MIO-16XE-50 Multipurpose I/0 Board. A Labview program is used for the testing records and displays all data acquired from the wind tunnel.

The measurement uncertainties were obtained from manufacturer specifications. These uncertainties are then propagated through the data reduction equations to give the uncertainties for the final results. The hygrometers used to measure dew point temperature are General Eastern models M1 and M4, both of which list an uncertainty of ±0.2°C. The pressure transducers are both a Setra model 239 which have an uncertainty of ±0.0007 inH2O. The coolant flow rate is measured with a Micro Motion mass flow sensor; model R050512390, which has a listed uncertainty of 0.5%. For the averaged thermopile measurements a conservative uncertainty of ±0.1°C is used. The RTDs used to measure the coolant temperature were given an uncertainty of ±0.05°C. The nozzle used to measure the air mass flow rate has an associated uncertainty of 2%. Other uncertainties propagated in the data reduction are correlation uncertainties. The uncertainty associated with the Gnielinski correlation was 10% based on the work of Shah [11].

2.2 Test Specimen

The test specimen used in this experiment is a plain fin-and-tube heat exchanger. A cross-section of the heat exchanger is given in Figure 2.2.1. The heat exchanger has two passes from eight tubes in a staggered arrangement. The tubes are made of copper with a 3/8” (9.525 mm) outer diameter. The fins on the heat exchanger are collared aluminum with a thickness of 0.102 mm and a spacing of 1.7 mm. This heat exchanger has 15 fins per

inch and the following overall dimensions: height 20.32 cm, width 23.50 cm, depth 4.45 cm, heat transfer surface area 2.13 m^2, minimum free flow area 0.028 m^2, and frontal area 0.045 m^2. The vortex generators used on the heat exchanger have a base length of 3 mm, a chord length of 3 mm, and an angle of attack of 45°.

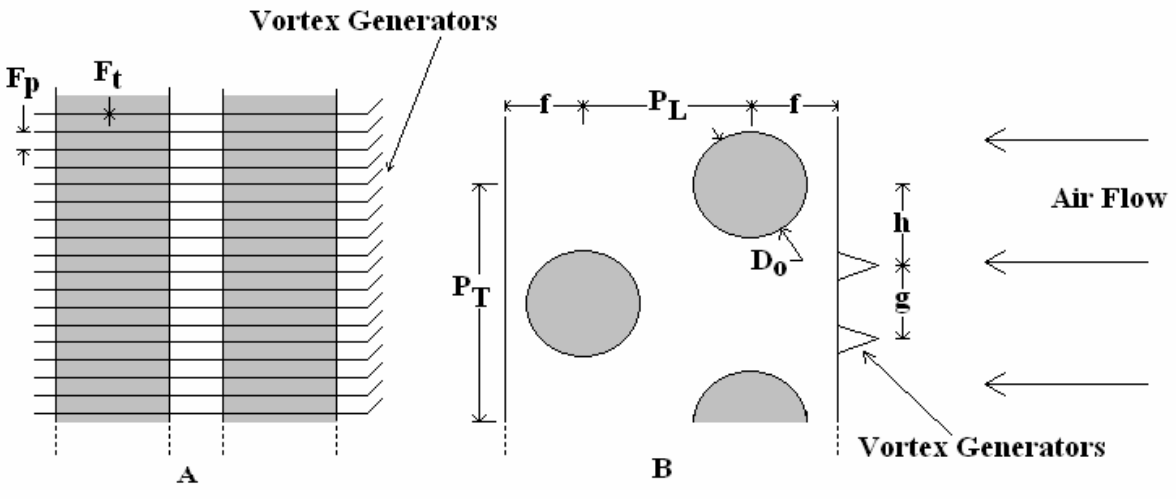

Figure 2.2.1 Cross-section of heat exchanger from side (A) and top (B) with vortex generators attached. Dimensions: F_P = 1.7 mm, F_t = 0.102 mm, P_L = 24 mm, P_T = 25 mm, f = 10 mm, g = 7 mm, h = 9 mm.

Chapter 3. Procedure

The heat exchanger was tested in the wind tunnel under both wet and dry conditions. A test was initiated by establishing steady-state conditions. The system was considered to be at steady-state when all temperature readouts had changed by less than 0.05°C in a one minute period. When steady-state is achieved, by obtaining 300 readings every two seconds, and the average of those samples is then recorded for every two second span over the five minutes recorded for each run. An energy balance is then performed to check the performance of the wind tunnel. The equations used to obtain the energy balance are given in Appendix A. The energy balance for all tests is given in Figure 3.1.1. 87% of the tests have an energy balance within ±5% between the calculated refrigerant and air-side heat transfer rates.

For testing in wet conditions, steam is added to the wind tunnel to increase the upstream dew point temperature. The humidity level is set such that the downstream dew point temperature is well above the exiting refrigerant temperature. This condition is set to ensure a fully wet condition on the heat exchanger. The wind tunnel is initially run in this condition for a few hours to ensure a steady condensate retention rate. Therefore, the rate of water condensation on the heat exchanger is balanced by the rate of condensate drainage.

Since a Wilson plot technique is used to determine air-side thermal resistance, the tests are grouped by air-side conditions. For each Wilson plot, the air-side properties are held constant while the tube-side refrigerant flow rate is increased. Each Wilson plot group has four to six runs measured. The heat exchanger was first tested without any modifications to determine its baseline performance. These tests were conducted at a variety of temperature and Reynolds number combinations that fell within a normal range of operation. The humidity level was controlled to include dry and fully wet conditions. The range of environmental conditions tested is included in Appendix A.

The heat exchanger was then modified by the addition of vortex generators. The vortex generators were placed at the leading edge of the heat exchanger with a nonconductive two-sided tape. Therefore, the available heat transfer surface area was unaffected. In total, 2100 vortex generators were placed on the heat exchanger. When this process was completed the same tests performed under baseline conditions were repeated.

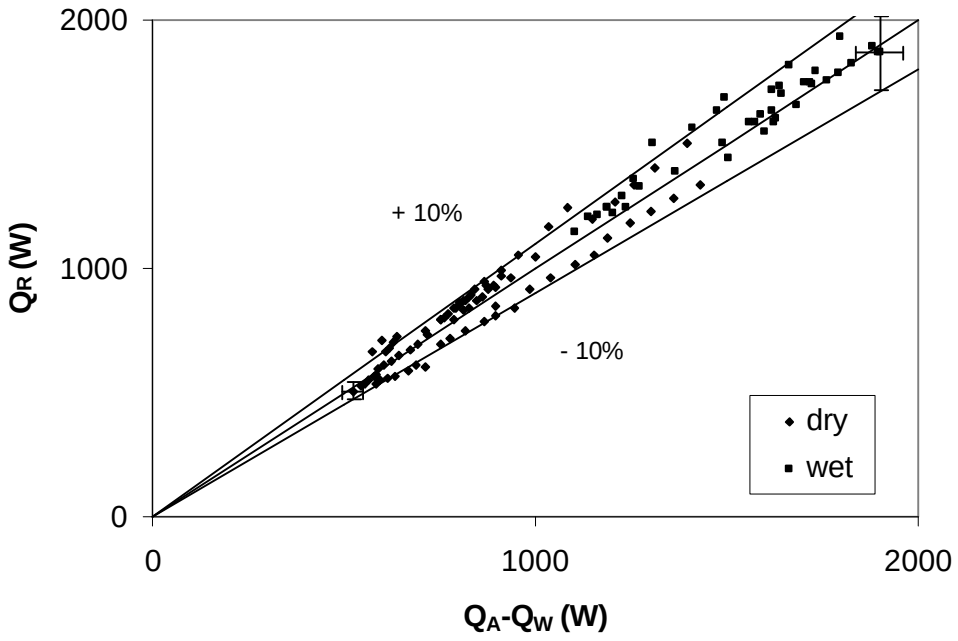

Figure 3.1 Energy balance for all tests performed.

Chapter 4. Results

4.1 Data Reduction

In order to evaluate the performance of a heat exchanger, the metric to be compared must be determined. The science of determining appropriate performance evaluation criteria (PEC) has been studied in literature [12]. The PEC chosen to evaluate the enhancement for this heat exchanger is a modified volume goodness factor, which will be discussed in detail later in this chapter. In order to reduce the error of the air-side convective heat transfer coefficient a Wilson plot technique is used to determine air-side thermal resistance. Therefore, a comparison of air-side thermal resistance is included in the data comparison. The art of thermal sciences has been developed primarily through correlations to empirical results. While these results may not directly express the fundamental physics of the relative phenomena, they are very useful in characterizing thermal systems. For our heat exchanger, correlations will be used to obtain the parameters necessary for our chosen comparisons. The uncertainties associated with the calculated quantities are determined using the method of Kline and McClintock [13] from the uncertainties associated with the measurements and the correlations.

A traditional metric for evaluating heat exchanger performance is the Area Goodness Factor (AGF). The AGF is measured as the ratio of the Colburn j factor (j) and the friction factor (f). This ratio is then typically plotted against the Reynolds number. The AGF directly relates dimensionless heat transfer and pressure drop. While this comparison is simple, its interpretation is not so straightforward. The difficulty in interpretation notwithstanding, this method provides a useful initial comparison. The volume goodness factor (VGF) compares the heat transfer enhancement per unit core volume to the required fan power per unit core volume. In the opinion of this researcher, this method better represents any benefit associated with this technique, because the interpretation of the results is more direct than those from an AGF comparison. Since correlations are easily obtainable for j and f in the literature an AGF comparison is performed on this heat exchanger and is included in Chapter 5. This method is used to compare a vortex generator enhancement technique to other enhanced surfaces by using published correlations for the j and f factors.

Air-Side Thermal Resistance

The Wilson plot technique removes the convective resistance on the refrigerant side of the thermal resistance network by extrapolating it to an infinite refrigerant flow velocity. In this method, the air-side operating conditions are held constant while the refrigerant flow rate is increased. Increasing the refrigerant flow rate decreases the refrigerant side convective resistance. Figure 4.1.1 shows the total thermal resistance network, neglecting any fouling resistance. The total resistance, or overall heat transfer coefficient, is determined as:

$$\frac{1}{UA} = R_{TOTAL} = R_{REFRIGERANT} + R_{CONDUCTION} + R_{AIR-SIDE} \tag{4.1}$$

where the refrigerant resistance is a convective resistance.

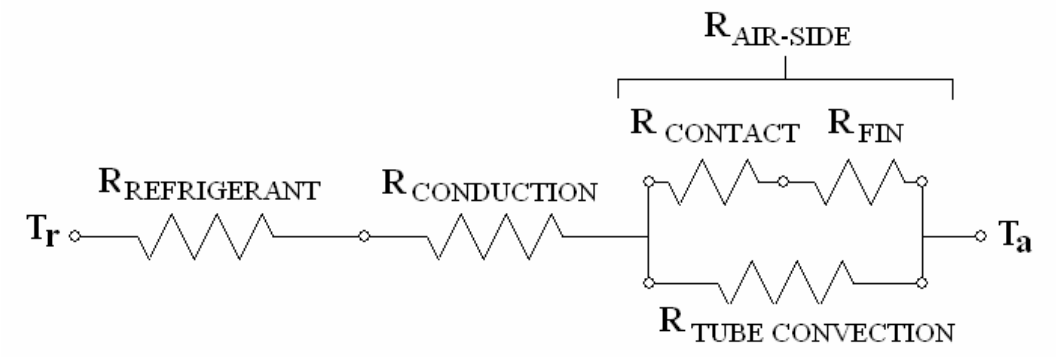

Figure 4.1.1 Resistance network for a heat exchanger.

The convective resistance for the refrigerant side can be expressed in terms of the Nusselt number as:

$$R_{REFRIGERANT} = \frac{CONSTANT}{Nu_D} \tag{4.2}$$

Equation (4.1) can now be rewritten as:

$$\frac{1}{U} = A_T\left(R_{CONDUCTION} + R_{AIR-SIDE}\right) + \frac{CONSTANT}{Nu_D} \tag{4.3}$$

The refrigerant-side Nusselt number is determined using Gnielinski's correlation [14], where $3000 < Re_D < 5 \times 10^6$ and $0.5 < Pr < 2000$.

$$Nu_D = \frac{\left(f/8\right)\left(\mathrm{Re}_D - 1000\right)\mathrm{Pr}}{1.07 + 12.7\left(f/8\right)^{1/2}\left(\mathrm{Pr}^{2/3} - 1\right)} \tag{4.4}$$

The friction factor inside the tube is determined from the Petukhov correlation [15], with $3000 < Re_D < 5 \times 10^6$.

$$f = \left(0.79\ln\left(\mathrm{Re}_D\right) - 1.64\right)^{-2} \tag{4.5}$$

The Reynolds number based on the tube diameter is defined as

$$\mathrm{Re}_D = \frac{4\dot{m}_R}{pDm_R} \tag{4.6}$$

where the refrigerant properties are evaluated from curve-fits to data provided by the manufacturer at the mean refrigerant temperature. The curve-fits used are included in the data reduction program in Appendix B. For dry tests the overall heat transfer coefficient is determined from the log-mean temperature difference and the average heat transfer rate:

$$U = \frac{Q_{AVG}}{F\Delta T_{LM} A_T} \tag{4.7}$$

The correction factor, F, is approximately 1 for the range of tested conditions using the correction factor plot for a single-pass, cross-flow heat exchanger [16]. The log-mean temperature difference is calculated as

$$\Delta T_{LM} = \frac{\left(T_{US,A} - T_{DS,R}\right) - \left(T_{DS,A} - T_{US,R}\right)}{\ln\left(\frac{T_{US,A} - T_{DS,R}}{T_{DS,A} - T_{US,R}}\right)} \tag{4.8}$$

and Q_{AVG} is evaluated as

$$Q_{AVG} = \frac{\left(Q_A - Q_W\right) + Q_R}{2} \tag{4.9}$$

The refrigerant side energy transfer is calculated assuming a constant specific heat for the refrigerant

$$Q_R = \dot{m}_R Cp_R \Delta T_R \tag{4.10}$$

and the air-side energy transfer is calculated by the enthalpy difference in the air-water mixture as

$$Q_A = \dot{m}_A \Delta I_A \tag{4.11}$$

and the energy transfer to condensate for wet testing conditions is calculated as

$$Q_W = \dot{m}_W h_W \tag{4.12}$$

For wet tests a similar procedure is used with the exception that a log-mean enthalpy difference is used instead of the log-mean temperature difference. The log-mean enthalpy difference method was adapted from Idem [17]. The log mean enthalpy difference is calculated as

$$\Delta I_{LM} = \frac{\left(I_{US,A} - I_{DS,S}\right) - \left(I_{DS,A} - I_{US,S}\right)}{\ln\left(\frac{I_{US,A} - I_{DS,S}}{I_{DS,A} - I_{US,S}}\right)} \tag{4.13}$$

where a fictitious saturation enthalpy is evaluated at the surface temperature. The surface temperature is estimated from the refrigerant-side convective resistance and the conductive resistance is neglected.

$$T_S = T_R + \frac{Q_{AVG}}{h_R A_R} \tag{4.14}$$

It is important to note that the convective resistance altered the surface temperature by as much as 4°C and should not be neglected. From these calculations the overall heat transfer coefficient is determined as

$$U = \frac{Q_{AVG}}{F \Delta I_{LM} A_T} \tag{4.15}$$

A Wilson plot is then constructed in the same manner as the dry tests.

For each Wilson plot the conductive and air-side resistances are held fixed; therefore, Equation (4.3) forms the equation of a line. The secondary effects of air-side conditions on the refrigerant side Nusselt number are neglected; thus, all the dry Wilson plot tests have a common slope and all of the wet Wilson plots have a common slope. A weighted least-squares method is then used on all the Wilson plots to determine the slope for the heat exchanger. The intercept is concurrently solved for each run and used to determine the air-side thermal resistance. The weighted least-square technique is desirable because the measurement uncertainty is not constant for each data

point. The tube area and the conduction resistance are then calculated in order to obtain the air-side thermal resistance. The weighted least-squares technique used here is derived in Appendix A.

For wet tests a comparison of the overall heat transfer coefficient with no refrigerant-side convective resistance will be presented. This 'raw' comparison makes data interpretation simple.

Area Goodness Factor

The Area Goodness Factor (AGF) is a commonly used tool to evaluate air-side heat transfer enhancement techniques. The AGF is defined as the Colburn *j* factor divided by the friction factor *f*. The Colburn j factor for heat transfer is given as:

$$j = St\,\mathrm{Pr}^{2/3} = \frac{h}{rVCp}\left(\frac{Cpm}{k}\right)^{2/3} \tag{4.16}$$

The intensive fluid properties for the air are evaluated at the average air temperature and average dew point temperature. The air-side convective heat transfer coefficient is determined from the air-side thermal resistance calculated in the Wilson plot tests,

$$h_A = \frac{1}{R_{AIR-SIDE} A_T h_O} \tag{4.17}$$

and the air-side friction factor is found from solving [15]

$$\Delta P = \frac{(rV)^2}{2r_{US}}\left[\left(1+\left[\frac{A_{FF}}{A_{FR}}\right]^2\right)\left(\frac{r_{US}}{r_{DS}}-1\right)+ f\,\frac{A_T}{A_{FF}}\frac{r_{US}}{r}\right] \tag{4.18}$$

Volume Goodness

The Volume Goodness factor compares the air-side heat transfer per unit core volume to the fan power required per unit core volume. The heat transfer per unit core volume is calculated as the product of the surface efficiency, the air-side convective heat transfer coefficient, and ß, which is the total heat transfer surface area per unit core volume as shown below.

$$Z = h_O h_A b \tag{4.19}$$

The air-side convective heat transfer coefficient is determined from the air-side thermal resistance as shown in Equation 4.13. The surface efficiency is determined from the fin efficiency which is derived in Appendix A. The fan power per unit core volume is calculated as the product of the pressure drop across the heat exchanger and the volumetric flow rate divided by the core volume of the heat exchanger.

$$E = \Delta P \frac{\dot{m}_A}{V r_A} b \tag{4.20}$$

4.2 Analysis

Figures 4.2.1 and 4.2.2 show the air-side thermal resistance for dry and wet testing conditions. The average reduction in air-side thermal resistance is 10% for dry tests and is consistent throughout the range of Reynolds numbers tested. In wet operating conditions the air-side thermal resistance increased at higher Reynolds numbers.

The resulting core pressure drop associated with this enhancement can be seen in Figures 4.2.3 and 4.2.4. The average corresponding increase in core pressure drop is 5% in dry conditions and within the experimental uncertainty for wet conditions.

Figure 4.2.5 shows the enhancement to the volume goodness factor due to the addition of vortex generators under dry operating conditions. From this figure it can be seen that there is a consistent enhancement present over the range of tested fan power. The average enhancement to the volume goodness factor in dry testing conditions is 10%. Figure 4.2.6 shows the effect on the overall heat transfer coefficient for wet testing conditions evaluated at zero refrigerant convective resistance. For wet operating conditions the vortex generators had an 8% reduction in the overall heat transfer coefficient.

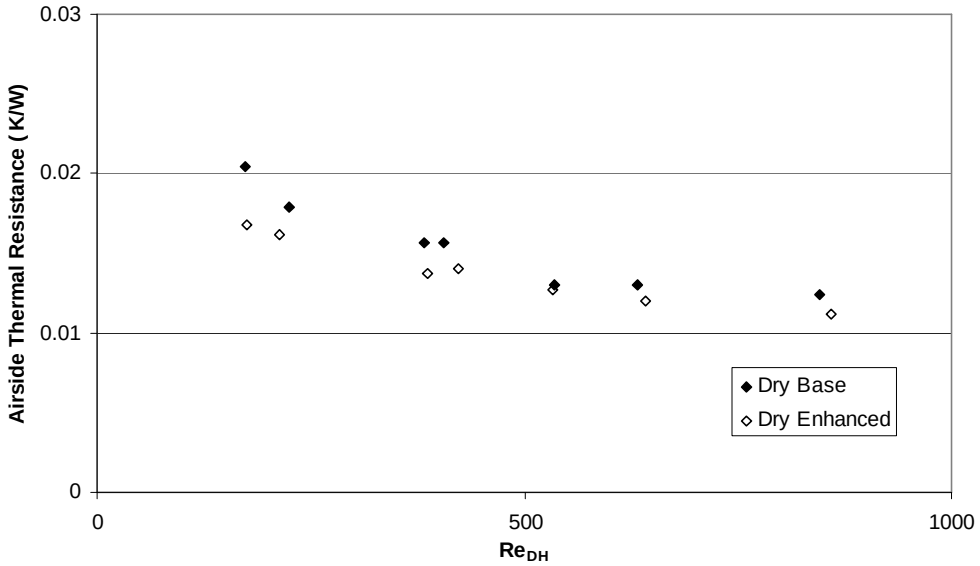

Figure 4.2.1 Air-side thermal resistance from Wilson plot technique for dry tests.

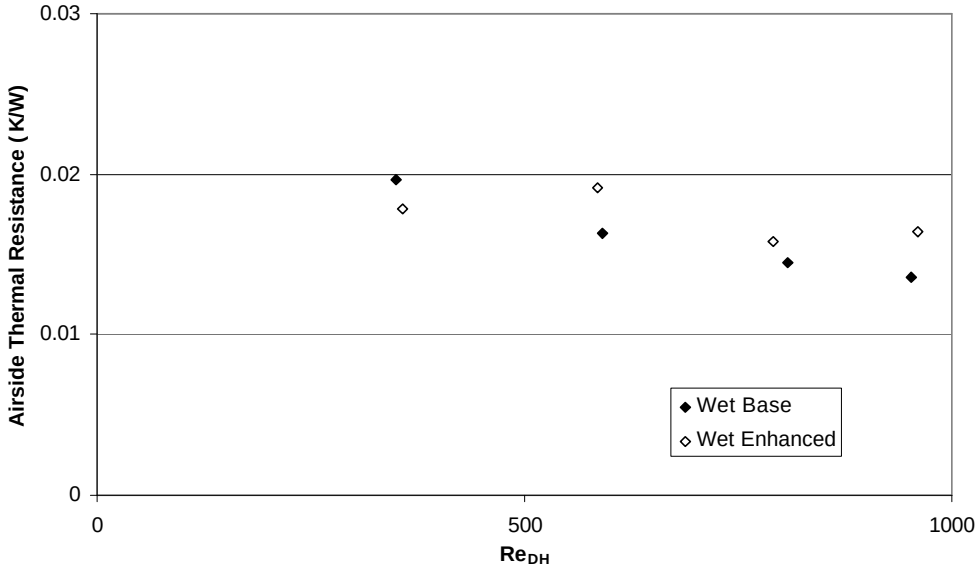

Figure 4.2.2 Air-side thermal resistance from Wilson plot technique for wet tests.

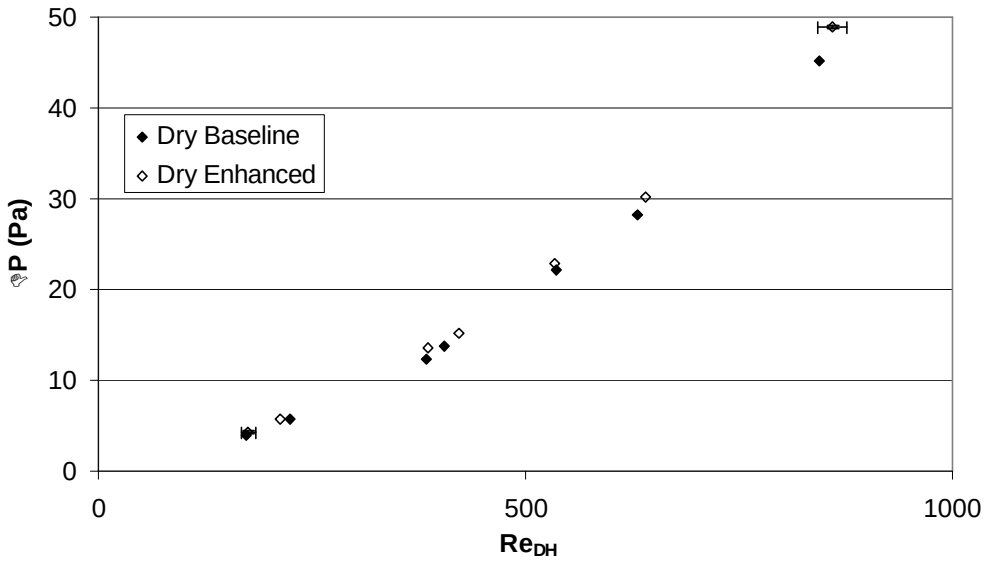

Figure 4.2.3 Air-side pressure drop across the heat exchanger for dry tests.

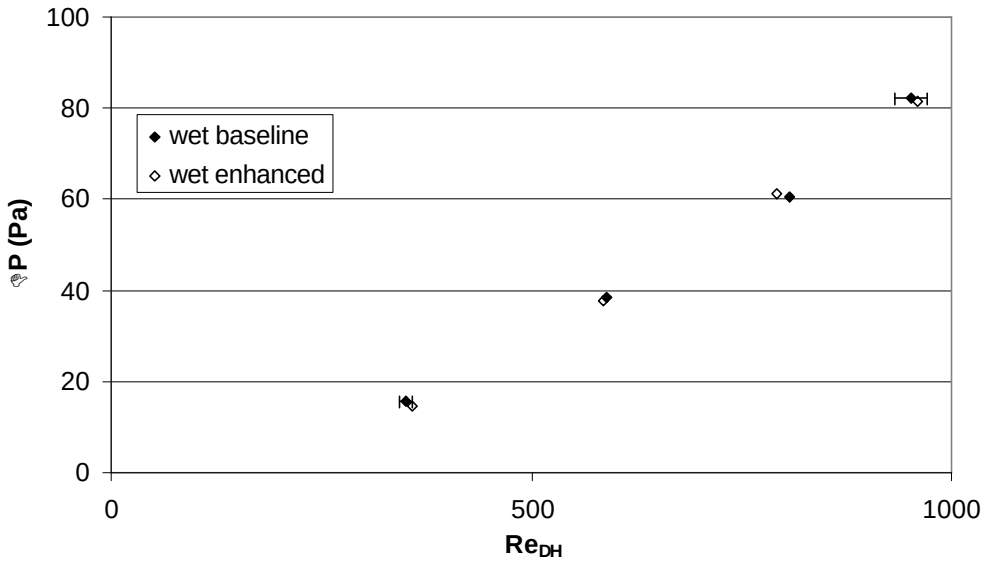

Figure 4.2.4 Air-side pressure drop across the heat exchanger for wet tests.

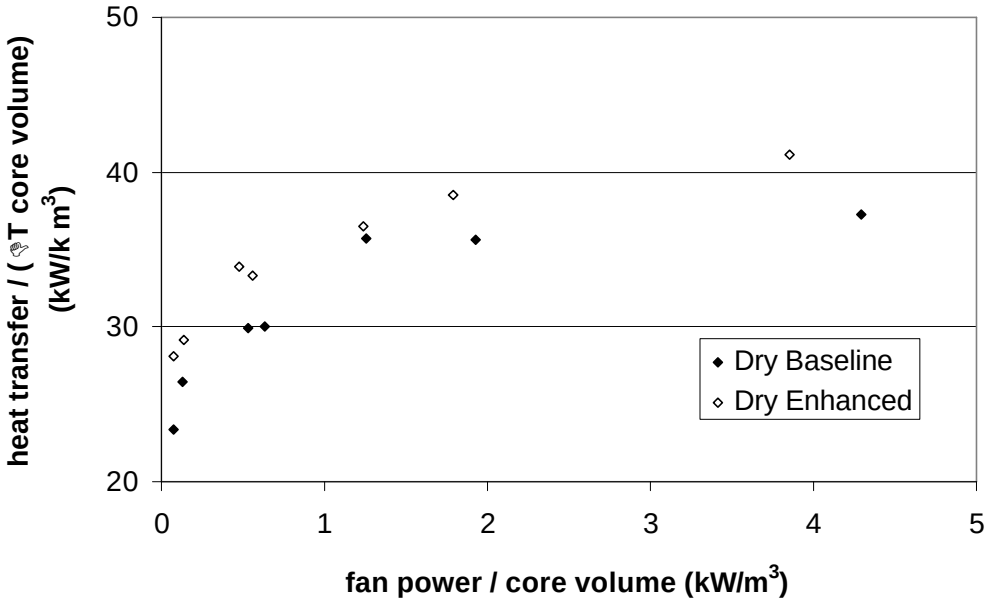

Figure 4.2.5 Dry volume goodness data for baseline and enhanced tests.

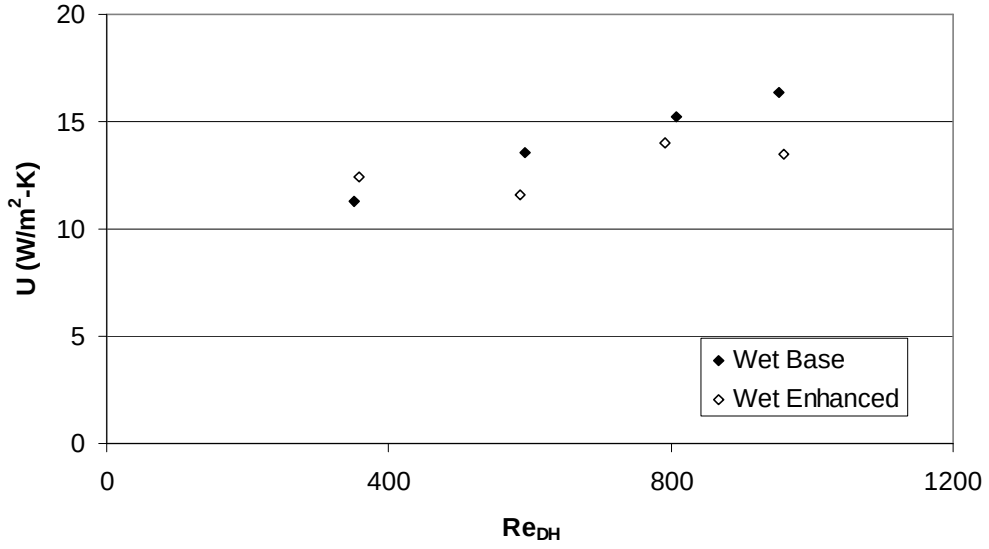

Figure 4.2.6 Wet overall heat transfer coefficient for baseline and enhanced tests.

Chapter 5. Comparison

An analysis was performed to compare vortex generator enhancement to other types of enhanced heat transfer surfaces. The Area Goodness Factor, developed in Chapter 4, will be used on the data obtained in the Wilson plot tests. Correlations from literature will be used to determine the Area Goodness Factor for other enhanced surfaces. Dimensions necessary for the correlations were chosen to keep as much dimensional similarity as possible for the various surfaces. The length scales used for the Reynolds number are different for the various correlations. Therefore, the j and f factors are first calculated based on the length scale necessary for the correlation, and then shifted to match the length scale for the vortex generator enhanced heat exchanger. A collection of j and f correlations is obtained from Park [18].

For dry conditions a slit-fin round-tube heat exchanger and a flat-tube, louvered-fin heat exchanger were chosen for a comparison. For the flat-tube louvered-fin heat exchanger the correlations used are presented by Wang and Chang (1997),

$$j = \mathrm{Re}_{Lp}^{-0.49}\left(\frac{q}{90}\right)^{0.27}\left(\frac{F_p}{L_p}\right)^{-0.14}\left(\frac{F_l}{L_p}\right)^{-0.29}\left(\frac{T_d}{L_p}\right)^{-0.23}\left(\frac{L_l}{L_p}\right)^{0.68}\left(\frac{T_p}{L_p}\right)^{-0.28}\left(\frac{d_f}{L_p}\right)^{-0.05} \tag{5.1}$$

$$f = f1 * f2 * f3 \tag{5.2}$$

$$f1 = 4.97\,\mathrm{Re}_{Lp}^{\left(0.6049-\frac{1.064}{q^{0.2}}\right)}\left(\ln\left(\left(\frac{d_f}{F_p}\right)^{0.5}+0.9\right)\right)^{-0.527} \tag{5.3}$$

$$f2 = \left(\left(\frac{D_h}{L_p}\right)\ln\left(0.3\mathrm{Re}_{Lp}\right)\right)^{-2.966}\left(\frac{F_p}{L_l}\right)^{-0.7931\left(\frac{T_p}{T_h}\right)} \tag{5.4}$$

$$f3 = \left(\frac{T_p}{D_m}\right)^{-0.0446}\ln\left(1.2+\left(\frac{L_p}{F_p}\right)^{1.4}\right)^{-3.553} q^{\,-0.477} \tag{5.5}$$

These correlations are valid over the compared range of Reynolds numbers tested. The louver pitch was set the same as the hydraulic diameter of the vortex generator enhanced heat exchanger; therefore, the length scales are the same for both sets of data. The slit-fin round tube heat exchanger correlations used is from Kim and Jacobi (2000) for uncoated surfaces.

$$j_{uncoated} = 0.3647\left(\mathrm{Re}_{Dc}\right)^{-0.1457}\left(\frac{F_p}{D_c}\right)^{1.21}\left(\frac{P_l N}{D_c}\right)^{-0.3181} \tag{5.6}$$

$$f_{uncoated} = 1.265\left(\mathrm{Re}_{Dc}\right)^{-0.2991}\left(\frac{F_p}{D_c}\right)^{-0.2918}\left(\frac{P_l N}{D_c}\right)^{-0.1985} \tag{5.7}$$

Figures 5.1 and 5.2 show the results from these correlations and the data obtained from the vortex generator enhanced heat exchanger.

For wet operating conditions, comparisons are made for vortex generator enhancement, round-tube louvered-fin, and a round-tube slit-fin heat exchanger. The correlations used for the round-tube louvered-fin arrangement come from Wang *et al.* (2000),

$$j = 9.717\,\mathrm{Re}_{Dc}^{J1}\left(\frac{F_p}{D_c}\right)^{J2}\left(\frac{P_l}{P_t}\right)^{J3}\ln\left(3-\frac{L_p}{F_p}\right)^{0.07162} N^{-0.543} \tag{5.8}$$

where,

$$J1 = -0.023634 - 1.2475\left(\frac{F_p}{D_c}\right)^{0.65}\left(\frac{P_l}{P_t}\right)^{0.2} N^{-0.18} \tag{5.9}$$

$$J2 = 0.856\exp(\tan q) \tag{5.10}$$

$$J3 = 0.25\ln(\mathrm{Re}_{Dc}) \tag{5.11}$$

and,

$$f = 2.814\,\mathrm{Re}_{Dc}^{F1}\left(\frac{F_p}{D_c}\right)^{F2}\left(\frac{P_l}{D_c}\right)^{F3}\left(\frac{P_l}{P_t}+0.091\right)^{F4}\left(\frac{L_p}{F_p}\right)^{1.958} N^{0.04674} \tag{5.12}$$

where,

$$F1 = 1.223 - 2.857\left(\frac{F_p}{D_c}\right)^{0.71}\left(\frac{P_l}{P_t}\right)^{-0.05} \tag{5.13}$$

$$F2 = 0.8079\ln(\mathrm{Re}_{Dc}) \tag{5.14}$$

$$F3 = 0.8932\ln(\mathrm{Re}_{Dc}) \tag{5.15}$$

$$F4 = -0.999\ln\left(\frac{2\Gamma}{m_f}\right) \tag{5.16}$$

$$\Gamma = \frac{\dot{m}}{WN}\text{: condensate flow rate per unit width per tube row} \tag{5.17}$$

The correlations used for the round-tube slit-fin heat exchanger come from Kim and Jacobi (2000),

$$j_{uncoated} = 0.3647(\mathrm{Re}_{Dc})^{-0.1457}\left(\frac{F_p}{D_c}\right)^{1.21}\left(\frac{P_l N}{D_c}\right)^{-0.3181} \tag{5.18}$$

$$f_{uncoated} = 1.265(\mathrm{Re}_{Dc})^{-0.2991}\left(\frac{F_p}{D_c}\right)^{-0.2918}\left(\frac{P_l N}{D_c}\right)^{-0.1985} \tag{5.19}$$

Figures 5.3 and 5.4 show the results from these correlations and the data obtained for the vortex generator enhanced heat exchanger.

In dry operating conditions Figure 5.2 shows a higher j/f value for the vortex generator enhanced surface in the lower range of Reynolds numbers. However, this advantage appears to drop as the Reynolds number increases. Since this comparison includes only two other types of enhanced heat transfer surfaces, it is important to realize that these two other surfaces are widely used in industry and that the vortex generator enhanced surface competes well in the operating range used for these experiments.

For the wet operating comparison, Figure 5.4 shows that the vortex generator enhanced surface has a consistent decrease in the j/f value as the Reynolds number increases. The round-tube louvered-fin correlation shows a higher j/f value for most of the range of Reynolds numbers. As with the dry comparisons, it is important to note that in wet operating conditions the vortex generator enhanced surface is comparable to the two other enhanced surfaces presented.

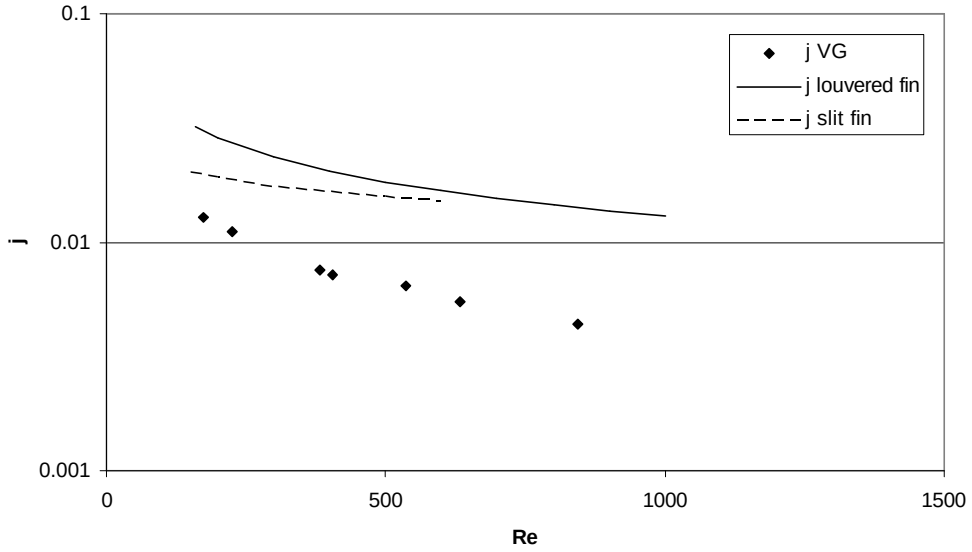

Figure 5.1 Colburn j factors for vortex generator and other enhanced surfaces for dry conditions.

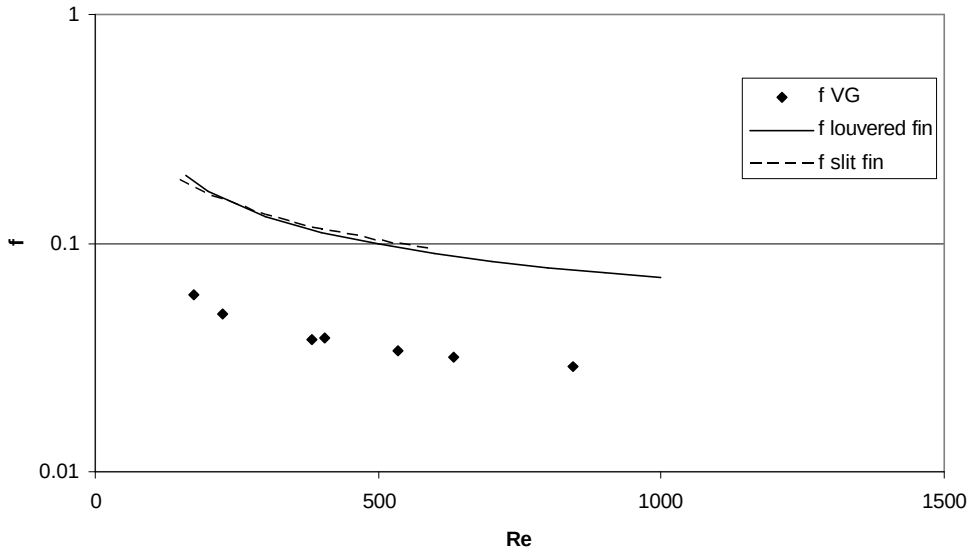

Figure 5.2 Friction factors for vortex generator and other enhanced surfaces for dry conditions.

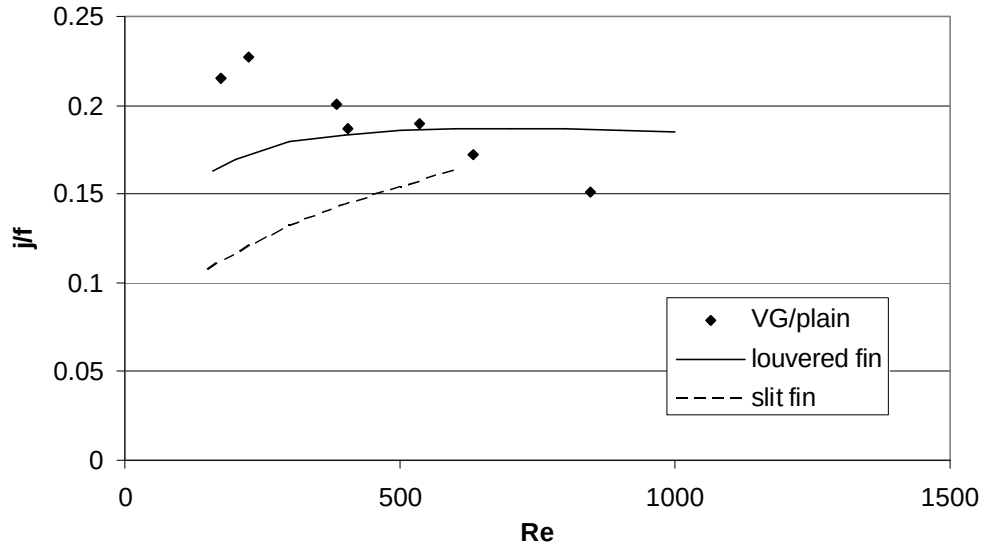

Figure 5.3 j/f for vortex generator and other enhanced surfaces for dry conditions.

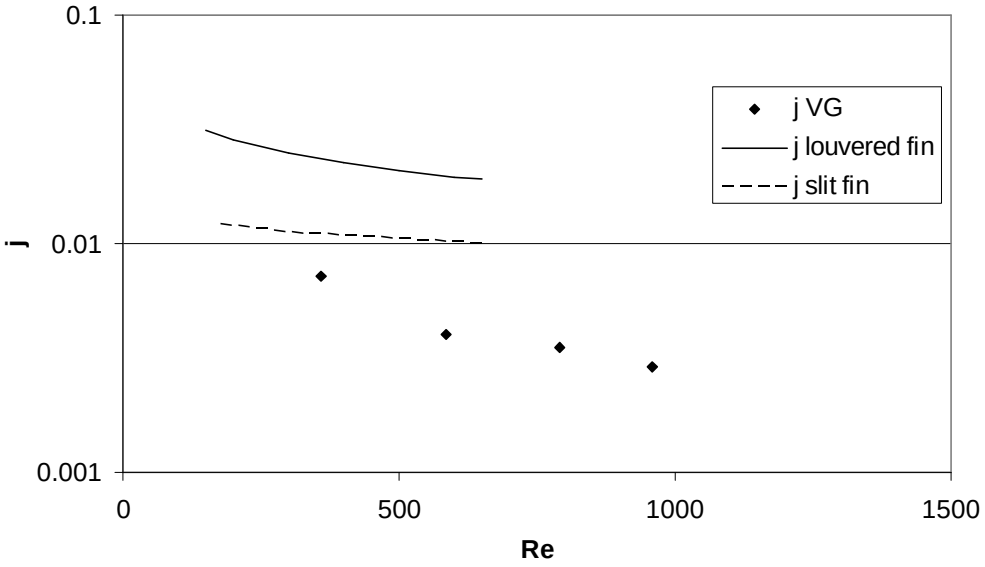

Figure 5.4 Colburn j factors for vortex generator and other enhanced surfaces for wet conditions.

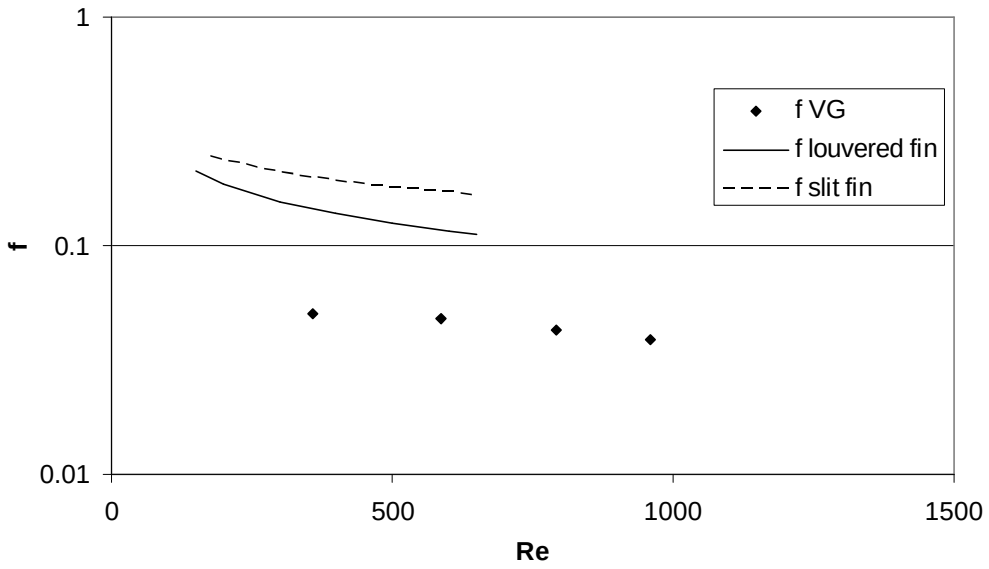

Figure 5.5 Friction factors for vortex generator and other enhanced surfaces for wet conditions.

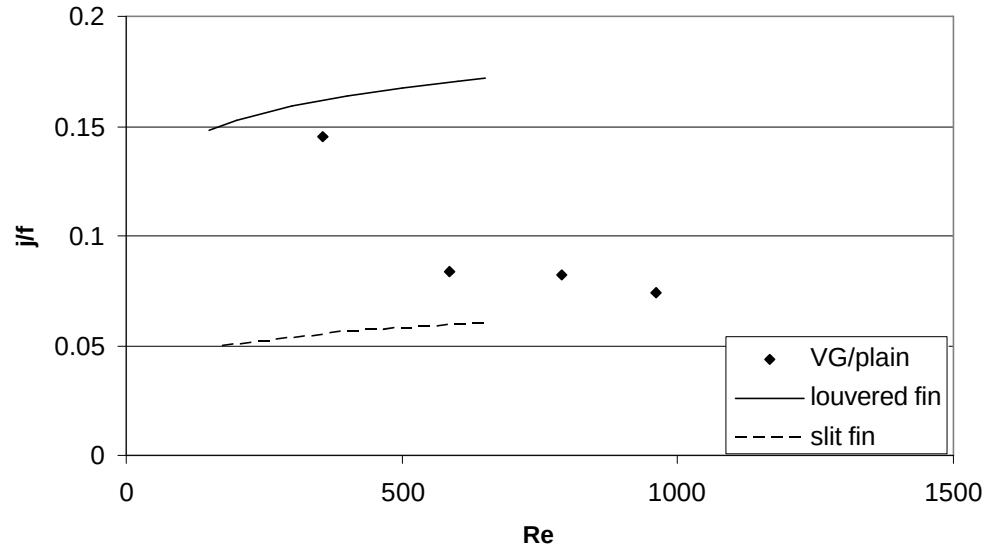

Figure 5.6 j/f for vortex generator and other enhanced surfaces for wet conditions.

Chapter 6. Summary and Conclusions

The goal of this study was to perform full scale testing for the application of vortex generators on a compact heat exchanger operating under both dry- and wet-surface conditions. The objective was to assess the viability of vortex generation as a heat transfer enhancement technique for such heat exchangers. A review of recent literature established the potential benefit for the use of vortex generation as a heat transfer enhancement technique. This review also showed a lack of both full-scale testing and especially testing with wet-surface conditions.

A plain fin-and-tube heat exchanger was obtained for testing. The baseline performance of this heat exchanger was obtained using a closed-loop wind tunnel. This heat exchanger was then augmented with 2100 vortex generators placed at the leading edges of the fins. The enhanced performance of the heat exchanger was then determined and compared to the baseline performance.

The addition of the vortex generators gave an average enhancement of 10% to the volume goodness factor under dry operating conditions. For wet operating conditions, a reduction in the overall enthalpy transfer coefficient was present over most of the Reynolds number range tested.

Using j and f correlations obtained from the literature, a comparison was made to other enhanced surfaces using the Area Goodness Factor. The comparison is made for both wet and dry results. The dry comparison shows a benefit for the vortex-generator enhanced heat exchanger in the lower range of Reynolds numbers tested. For both wet and dry tests the performance is comparable to other enhanced surfaces.

Vortex generation is a viable method of heat transfer enhancement. Vortex generation can be added to other standard enhancement techniques such as increasing the surface area, increasing the length of air pathlines, and other methods of reducing the thermal boundary layer thickness, to enhance the heat transfer of a heat exchanger. Much like other enhancement techniques, vortex generator enhancement diminishes under wet-surface operating conditions. This reduction in enhancement is comparable to the performance reduction of other enhancement techniques.

There are some areas where future research is needed to fully exploit the benefits of vortex generation as a method of heat transfer enhancement. This research focused on the enhancement of a plain fin-and-tube heat exchanger, but testing should also be performed to see if vortex generation may be incorporated with other enhancement techniques. Testing also needs to be performed on a full scale heat exchanger with internal vortex generators to determine the enhancement at other placements than the leading edge. Research is also needed to determine the behavior of the vortices with wet surface conditions. This study would establish the cause of the behavior under wet operating conditions.

References

1. Jacobi, A.M. and R.K. Shah, "Heat Transfer Surface Enhancement through the Use of Longitudinal Vortices: A Review of Recent Progress," *Experimental Thermal and Fluid Science*, 11, 295-309, 1995.
2. Fiebig, M. "Vortex generators for compact heat exchangers," *Journal of Enhanced Heat Transfer*, 2(1-2), 43-61, 1995
3. Fiebig, M. "Wing-type vortex generators (WVGS) heat transfer enhancement mechanisms and potential for heat transfer surfaces and heat exchangers," *Heat and Technology*, 15(1), 31-41, 1997
4. Torii, K., J.I. Yanagihara, and Y. Nagai, "Heat Transfer Enhancement by Vortex Generators," *Proceedings of The ASME/JSME Thermal Engineering Joint Conference*, 10309C, 77-83, 1991.
5. Kwak, K.M., K. Torii, and K. Nishino, "Heat transfer and flow characteristics of fin-tube bundles with and without winglet type vortex generators," *Experiments in Fluids*, v. 33, 696-702, 2002.
6. Fiebig, M., A. Valencia, and N. K. Mitra, "Wing type vortex generators for fin-and-tube heat exchangers," *Experimental Thermal and Fluid Science*, v. 7(4), 287-295, 1993.
7. Brockmeier, U. Guentermann, TH. Fiebig, M., "Performance evaluation of a vortex generator heat transfer surface and comparison with different high performance surfaces," *International Journal of Heat and Mass Transfer*. v 36 (10), 2575-2587, Jul 1993.
8. Chen, Y., M. Fiebig, and N. K. Mitra, "Heat transfer enhancement of finned oval tubes with staggered punched longitudinal vortex generators," *International Journal of Heat and Mass Transfer*, v 43 (3), 417-435, 2000.
9. Gentry, M.C. and A.M. Jacobi, "Heat Transfer Enhancement Using Tip and Junction Vortices," Air Conditioning and Refrigeration Center, ACRC Report TR-137, University of Illinois, Urbana 1998.
10. ElSherbini, A.I. and A.M. Jacobi, "An experimental evaluation of the thermal-hydraulic impact of delta-wing vortex generators in plain-fin-and-tube heat exchangers," Air Conditioning and Refrigeration Center, ACRC Report TR-172, University of Illinois, Urbana 2000.
11. Bhatti, M.S., and R.K. Shah, "Turbulent and Transition Flow Convective Heat Transfer in Ducts," *Handbook of Single-phase Convective Heat Transfer*, S. Kakac, R.K. Shah, and W. Aung, eds. Wiley, New York, 1987.
12. Pira, J., C. W. Bullard and A.M. Jacobi, "An Evaluation of Heat Exchangers Using System Information and PEC," Air Conditioning and Refrigeration Center, ACRC Report TR-175, University of Illinois, Urbana 2000.
13. Kline, S.J., and F. A. McClintock, "Describing experimental uncertainties in single sample experiments," *Mechanical Engineering*, 75, 3-8, 1953.
14. Gnielinski, V., "New equations for heat and mass transfer in turbulent pipe and channel flow," *International Chemical Engineering*, 16, 359-368, 1976.
15. Petukhov, B.S., *Advances in Heat Transfer*, T.F. Irvine and J.P. Hartnett, Eds ,v. 6, Academic Press, New York, 1970.
16. Incropera, F.P. and D.P. Dewitt, *Fundamentals of Heat and Mass Transfer, 4th ed*, John Wiley and Sons, New York, 1996.
17. Idem, Stephen A., "An Instantaneous Condensing Gas-fired Water Heater: Modeling and Performance," Herrick Lab Report 0564-5, Purdue University, West Lafayette, Indiana, 1984.
18. Park, Young-Gil, "Air-Side Performance Characteristics of Round- and Flat-Tube Heat Exchangers: A Literature Review, Analysis and Comparison," ACRC Report CR-36, University of Illinois, Urbana, 2001.
19. Kern, D.Q., and D.A. Kraus, *Extended Surface Heat Transfer*, McGraw-Hill, New York, 1972.
20. ARI, *Standard for Forced-Circulation Air-Cooling and Air-Heating Coils*, ARI-410.

Appendix A

A.1 Energy Balance

An energy balance is used to express the validity of the measurements taken in the experiments. The energy balance compares the calculated air-side heat transfer rate to the refrigerant-side heat transfer rate. The sensible air-side heat transfer rate is calculated as the condensate energy subtracted from the total heat transfer.

$$Q_A = \dot{m}_A \Delta h_A \tag{A.1}$$

$$Q_W = m_w h_w \tag{A.2}$$

The refrigerant-side heat transfer rate is calculated assuming a constant specific heat evaluated at the average refrigerant temperature.

$$Q_R = \dot{m}_R Cp_R \Delta T_R \tag{A.3}$$

A plot of the calculated air-side and refrigerant-side heat transfer rates is included in Chapter 3. The results of the energy balance analysis are also presented in Chapter 3.

A.2 Testing Conditions

The environmental conditions for each Wilson Plot test are given in the table below.

Table A.2 Environmental operating conditions.

	Upstream air temperature (°C)	Inlet coolant temperature (°C)	Upstream dew point temperature (°C)	Face Velocity (m/s)
Dry Baseline	26.9	10.4	10.5	2.9
	27.4	10.9	10.5	6.0
	30.4	8.2	7.5	4.5
	36.1	6.6	5.8	4.0
	32.8	11.9	5.3	1.2
	32.9	12.1	5.1	2.7
	39.5	12.1	5.8	1.7
Dry Enhanced	26.7	10.4	2.0	2.9
	27.7	10.6	1.2	6.0
	30.1	8.7	0.6	4.5
	36.4	6.8	1.2	3.9
	34.3	11.4	3.2	1.3
	33.0	12.2	4.2	2.8
	40.4	11.5	5.2	1.6
Wet Baseline	35.1	3.8	17.9	4.3
	35.0	4.6	20.3	5.9
	34.8	4.7	20.3	7.0
	34.5	1.9	16.3	2.5
Wet Enhanced	34.7	1.4	20.4	4.3
	34.6	1.8	19.8	5.8
	34.8	4.7	20.3	7.0
	34.8	1.9	15.1	2.6

A.3 Weighted Least-Squares Reduction

For the Wilson plot technique a weighted least-squared error (WLSE) method is used to determine the slope and intercept for the data provided. The WLSE technique accounts for the uncertainty associated with the variables. The form of the function desired is know to be linear, this gives the WLSE the following form,

$$\sum_{i=1}^{n}\left(\frac{a+bx_i-y_i}{s_i}\right)^2 \rightarrow \text{minimum}$$

$$x_i = \frac{1}{Nu_D}, \qquad y_i = \frac{1}{U}, \text{and} \tag{A.4}$$

s_i = uncertainty

This minimum is found by taking the derivative with respect to *a* and *b*, setting these equations equal to zero, and then solving the set of equations. The resulting set of equations is

$$a\sum_{i=1}^{n}\frac{1}{s_i^2}+b\sum_{i=1}^{n}\frac{x_i}{s_i^2}=\sum_{i=1}^{n}\frac{y_i}{s_i^2} \tag{A.5}$$

$$a\sum_{i=1}^{n}\frac{x_i}{s_i^2}+b\sum_{i=1}^{n}\frac{x_i^2}{s_i^2}=\sum_{i=1}^{n}\frac{x_i y_i}{s_i^2} \tag{A.6}$$

The slope was determined to be constant in Chapter 4; therefore, the variable b is the same for each Wilson plot. To solve for this common slope Equations A.4 and A.5 are written for each Wilson plot set and solved simultaneously, with the slope declared as the same variable in each equation. A sample of Wilson plots are presented in Figure A.3.1.

A.4 Surface Efficiency

The surface efficiency is determined from the fin efficiency [16] as,

$$h_O = 1-\frac{A_F}{A_T}\left(1-h_F\right) \tag{A.7}$$

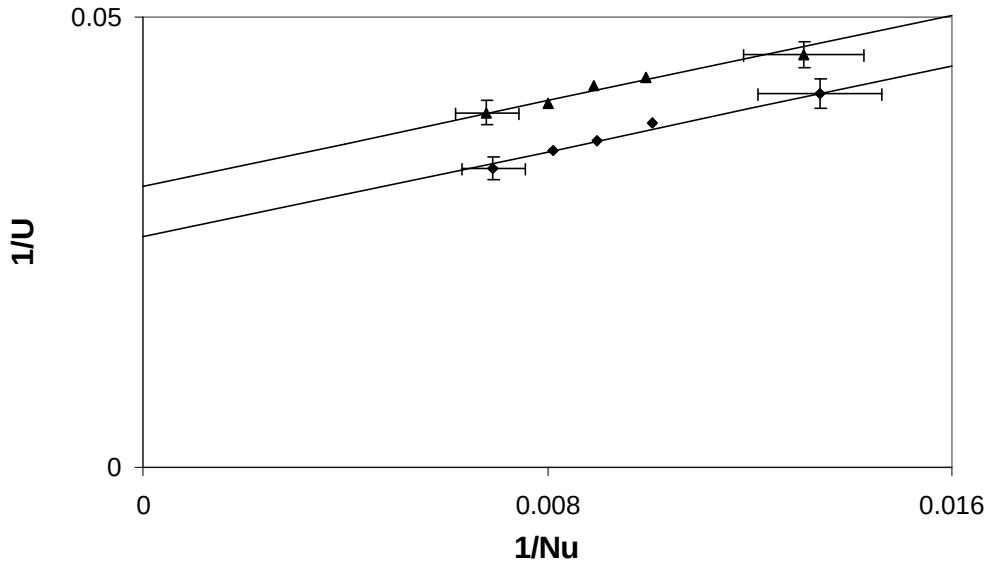

Figure A.3.1 Wilson Plot sets with WLSE fit extrapolated.

The fin efficiency is determined from the sector method. This sector method is similar to that used by Pira [11]. The sector method partitions the fin into hexagonal areas around each tube. These hexagonal areas are divided into sectors which are approximated with an equivalent radius. From this radius a radius ratio, R_N, and surface area, S_N, are calculated. The radius ratio and surface area are the used to determine the fin efficiency [19]. The inner radius used in this technique is determined using the equation recommended by ARI Standard 410 [20].

$$r_i = \frac{D_O - 2F_T}{2} = \frac{D_C}{2} \tag{A.8}$$

The numbers of sections chosen affect the accuracy of the sector method. For this experiment 32 sections are chosen and are categorized into 8 zones. A diagram showing the sectors is given in Figure A.3.1.

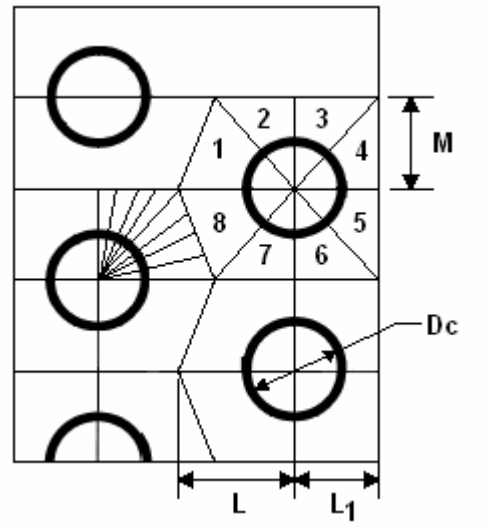

Figure A.3.2 Schematic of sector method used to calculate fin efficiency.

For zones 2, 3, 6, and 7 the radius ratio and surface area are determined as

$$R_n = \frac{M}{r_i}\sqrt{\left(\frac{2n-1}{2N}\right)^2 + \left(\frac{L}{M}\right)^2} \tag{A.9}$$

$$S_n = \frac{r_i^2}{2}\left(R_n^2 - 1\right)\left[\tan^{-1}\left(\frac{nM}{NL}\right) - \tan^{-1}\left(\frac{(n-1)M}{NL}\right)\right] \tag{A.10}$$

For zones 1 and 8 the radius ratio and surface area are determined as

$$R_n = \frac{M}{r_i}\sqrt{\left(\frac{2n-1}{2N}\right)^2\left(\frac{L}{M}\right)^2 + 1} \tag{A.11}$$

$$S_n = \frac{r_i^2}{2}\left(R_n^2 - 1\right)\left[\tan^{-1}\left(\frac{nL}{NM}\right) - \tan^{-1}\left(\frac{(n-1)L}{NM}\right)\right] \tag{A.12}$$

For zones 4 and 5 the radius ratio and surface area are determined as

$$R_n = \frac{M}{r_i}\sqrt{\left(\frac{2n-1}{2N}\right)^2 + \left(\frac{L_1}{M}\right)^2} \tag{A.13}$$

$$S_n = \frac{r_i^2}{2}\left(R_n^2 - 1\right)\left[\tan^{-1}\left(\frac{nM}{NL_1}\right) - \tan^{-1}\left(\frac{(n-1)M}{NL_1}\right)\right] \tag{A.14}$$

From these values the fin efficiency is then determined using the method presented by Kern and Kraus [17],

$$h_n = \frac{2r_i}{m\left(r_o^2 - r_i^2\right)}\left[\frac{K_1(mr_i)I_1(mr_o) - K_1(mr_o)I_1(mr_i)}{K_1(mr_o)I_0(mr_i) + K_0(mr_i)I_1(mr_o)}\right] \tag{A.15}$$

where K_n and I_n are modified Bessel functions and,

$$m = \sqrt{\frac{2h_A}{k_f F_t}} \tag{A.16}$$

The total fin efficiency is then calculated for the total fin surface area by the following average,

$$h_F = \frac{\sum_{n=1}^{N} S_n h_n}{\sum_{n=1}^{N} S_n} \tag{A.17}$$

A.5 Input Values

Table A.5.1 A list of all input test values.

T_A up	T_A down	Refrig. flow rate	T_R in	T_R out	DP heat exchanger	T dewpt. up	T dewpt. down	$\dot{m}_A$	$\dot{m}_R$
°C	°C	lbm/min	°C	°C	inH2O	°C	°C	kg/s	kg/s
dry base									
27.02	20.75	17.25	10.4	11.59	0.05526	10.5	10.5	0.09064	0.1304
26.89	20.48	19.9	10.42	11.47	0.05518	10.45	10.45	0.09054	0.1504
26.86	20.25	22.53	10.32	11.26	0.05525	10.47	10.47	0.09062	0.1703
26.82	20.01	26.13	10.3	11.13	0.05534	10.39	10.39	0.09082	0.1975
26.87	19.69	32.76	10.32	11.01	0.05527	10.48	10.48	0.09088	0.2477
26.85	19.46	38.07	10.36	10.97	0.05536	10.47	10.47	0.09105	0.2878
26.82	19.17	45.44	10.43	10.94	0.0551	10.48	10.48	0.09078	0.3435
27.53	23.68	17.3	10.8	12.33	0.183	10.48	10.48	0.1906	0.1308
27.44	23.45	20.3	10.8	12.15	0.182	10.49	10.49	0.19	0.1535
27.39	23.23	24.58	10.89	12.05	0.1832	10.5	10.5	0.1911	0.1858
27.34	22.93	31.57	10.99	11.94	0.1845	10.48	10.48	0.1921	0.2387
27.28	22.72	36.36	11	11.85	0.1832	10.49	10.49	0.1913	0.2749
27.18	22.17	49.15	11.16	11.81	0.1714	10.25	10.25	0.1842	0.3716
29.86	23.75	17.31	8.12	9.992	0.1145	7.5	7.5	0.1433	0.1309
30.6	23.83	21.94	8.071	9.674	0.1124	7.44	7.44	0.1416	0.1659
30.65	23.56	26.79	8.094	9.471	0.1135	7.43	7.43	0.1427	0.2025
30.55	22.99	36.34	8.211	9.284	0.1132	7.45	7.45	0.1427	0.2747
30.57	22.69	43.9	8.348	9.265	0.1132	7.48	7.48	0.1429	0.3319
36.26	26.75	17.33	6.538	9.022	0.08958	5.8	5.8	0.1219	0.1310
36.16	26.16	21.97	6.525	8.588	0.08902	5.77	5.77	0.1218	0.1661
36.09	25.68	26.83	6.57	8.326	0.08925	5.76	5.76	0.122	0.2028
36.02	25.15	33.18	6.659	8.137	0.08903	5.76	5.76	0.1221	0.2508
36.01	24.59	42.46	6.85	8.058	0.08924	5.77	5.77	0.1224	0.3210
32.81	19.62	20.17	11.83	12.69	0.0161	5.23	5.229	0.03899	0.1525
32.77	19.01	26.57	11.81	12.47	0.01606	5.322	5.321	0.03899	0.2009
32.81	18.76	29.73	11.83	12.42	0.01599	5.276	5.275	0.03889	0.2248
32.82	18.56	32.84	11.83	12.37	0.01597	5.232	5.231	0.03889	0.2483
32.86	18.26	39.07	11.9	12.35	0.01593	5.23	5.229	0.03885	0.2954
32.84	18.11	41.97	11.91	12.33	0.01594	5.198	5.197	0.0389	0.3173
32.56	24.03	20.14	11.95	13.23	0.04966	5.027	5.025	0.08623	0.1523
32.74	23.66	26.54	12.04	13.06	0.04952	5.045	5.043	0.08626	0.2006
32.91	23.57	29.7	12.1	13.03	0.04961	5.114	5.112	0.08638	0.2245
33.07	23.48	32.8	12.13	12.99	0.04958	5.152	5.15	0.08644	0.2480
33.06	23.17	39.05	12.22	12.96	0.04943	5.201	5.199	0.08627	0.2952
39.16	23.89	20.13	12.02	13.36	0.02313	5.735	5.734	0.05106	0.1522
39.44	23.26	26.53	12.04	13.1	0.02294	5.762	5.761	0.05088	0.2006
39.66	23.06	29.7	12.1	13.06	0.0229	5.814	5.813	0.05084	0.2245
39.7	22.84	32.8	12.13	13.01	0.0229	5.857	5.856	0.05085	0.2480
39.59	22.39	39.07	12.22	12.97	0.02294	5.894	5.893	0.05098	0.2954

T_A up	T_A down	Refrig. flow rate	T_R in	T_R out	DP heat exchanger	T dewpt. up	T dewpt. down	$\dot{m}_A$	$\dot{m}_R$
°C	°C	lbm/min	°C	°C	inH2O	°C	°C	kg/s	kg/s
dry enhanced									
26.82	20.64	17.28	10.37	11.68	0.06089	2.132	2.13	0.09425	0.1306
26.72	20.42	19.59	10.35	11.54	0.06092	2.132	2.13	0.09441	0.1481
26.67	20.16	22.54	10.32	11.38	0.06089	2.106	2.104	0.09441	0.1704
26.69	19.97	26.12	10.29	11.24	0.061	2.106	2.104	0.09461	0.1975
26.63	19.61	32.74	10.36	11.14	0.06082	2.085	2.083	0.09452	0.2475
26.61	19.36	38.04	10.4	11.1	0.0605	1.863	1.861	0.09442	0.2876
26.67	19.18	44.97	10.5	11.12	0.06059	1.582	1.58	0.0945	0.3400
27.82	23.82	17.21	10.42	12.18	0.1995	1.36	1.353	0.1946	0.1301
27.71	23.6	20.19	10.51	12.08	0.1995	1.235	1.228	0.195	0.1526
27.69	23.34	24.42	10.54	11.9	0.1952	1.106	1.099	0.1924	0.1846
27.59	23	31.34	10.63	11.76	0.1957	1.008	1.001	0.193	0.2369
27.61	22.84	36.08	10.73	11.75	0.1955	0.9978	0.991	0.1929	0.2728
27.62	22.5	48.76	11	11.82	0.1947	1.266	1.259	0.1927	0.3686
30.31	24.31	17.22	8.724	10.8	0.1202	0.1706	0.1665	0.1432	0.1302
30.14	23.88	21.71	8.778	10.53	0.1208	0.4611	0.4569	0.1437	0.1641
30.11	23.55	26.45	8.803	10.33	0.1211	0.6661	0.6619	0.1439	0.2000
30.01	22.94	35.95	8.595	9.835	0.1211	0.8217	0.8175	0.1443	0.2718
30.03	22.64	43.42	8.634	9.728	0.1212	0.9432	0.939	0.1445	0.3283
36.67	27.28	17.2	6.812	9.489	0.09205	1.224	1.221	0.1207	0.1300
36.44	26.58	21.72	6.665	8.905	0.09183	1.193	1.19	0.1209	0.1642
36.35	26.11	26.45	6.684	8.615	0.09187	1.214	1.211	0.1211	0.2000
36.33	25.64	32.67	6.811	8.461	0.09172	1.238	1.235	0.1212	0.2470
36.3	24.97	41.96	6.816	8.193	0.09167	1.131	1.128	0.1213	0.3172
34.28	19.9	20.05	11.3	12.56	0.01719	2.978	2.977	0.03922	0.1516
34.31	19.34	26.43	11.3	12.33	0.0172	3.092	3.091	0.03936	0.1998
34.28	19.11	29.57	11.43	12.29	0.01724	3.208	3.207	0.03948	0.2235
34.4	18.95	32.66	11.49	12.28	0.01719	3.251	3.25	0.0394	0.2469
34.32	18.62	38.89	11.56	12.25	0.01722	3.307	3.306	0.03952	0.2940
34.37	18.47	41.77	11.59	12.25	0.01716	3.347	3.346	0.03943	0.3158
33.01	24.36	20.04	12.02	13.55	0.05427	3.935	3.933	0.08663	0.1515
32.95	23.85	26.36	12.08	13.33	0.05433	4.032	4.03	0.08683	0.1993
33	23.67	29.53	12.15	13.29	0.05441	4.143	4.141	0.08704	0.2232
33.04	23.51	32.62	12.2	13.27	0.05448	4.281	4.279	0.08711	0.2466
32.93	23.17	38.84	12.3	13.23	0.05448	4.392	4.39	0.08715	0.2936
40.19	23.44	20.09	11.43	13.03	0.02279	5.078	5.077	0.04845	0.1519
40.36	22.82	26.49	11.48	12.76	0.02271	5.146	5.145	0.04843	0.2003
40.4	22.61	29.64	11.52	12.7	0.0227	5.205	5.204	0.04845	0.2241
40.53	22.49	32.72	11.56	12.65	0.02271	5.279	5.278	0.04849	0.2474
40.49	22.02	38.91	11.63	12.58	0.02266	5.375	5.374	0.04849	0.2942
wet base									
35.19	25.83	20.35	3.502	6.231	0.1616	16.67	15.69	0.1313	0.1538
34.95	24.75	26.78	3.221	5.381	0.1547	18.21	18.55	0.1335	0.2025
35.16	24.7	29.96	3.128	5.139	0.1498	17.16	17.36	0.1361	0.2265

T_A up	T_A down	Refrig. flow rate	T_R in	T_R out	DP heat exchanger	T dewpt. up	T dewpt. down	$\dot{m}_A$	$\dot{m}_R$
°C	°C	lbm/min	°C	°C	inH2O	°C	°C	kg/s	kg/s
35.22	24.95	33.1	4.573	6.466	0.1607	19.64	19.39	0.1324	0.2502
35.15	24.4	39.34	4.591	6.241	0.1542	17.74	17.65	0.1331	0.2974
35.65	27.87	20.36	4.068	7.058	0.2393	22.03	21.82	0.1818	0.1539
35.15	27.13	26.82	4.24	6.679	0.2445	21.3	21.02	0.1833	0.2028
35.04	26.81	30.02	5.087	7.279	0.2503	21.43	21.18	0.1776	0.2270
34.64	26.29	33.14	4.711	6.718	0.2411	18.79	18.66	0.1845	0.2505
34.6	26.06	39.42	5.061	6.833	0.2369	17.83	17.76	0.1867	0.2980
34.89	28.06	20.34	3.709	6.766	0.3156	21.17	21.02	0.2147	0.1538
34.79	27.58	26.82	4.415	6.921	0.3452	22.32	22.1	0.2124	0.2028
34.6	27.21	30.03	4.775	7.014	0.3386	19.49	19.33	0.2154	0.2270
34.68	27.17	33.18	5.052	7.129	0.3321	18.3	18.18	0.2173	0.2508
35	27.38	39.41	5.602	7.481	0.3211	20.12	19.96	0.2184	0.2979
34.79	21.09	20.38	1.569	3.845	0.06276	16.69	16.57	0.0794	0.1541
34.61	20.65	26.87	1.94	3.718	0.06312	17.76	17.29	0.07765	0.2031
34.26	19.83	30.06	1.84	3.402	0.06201	16.01	15.71	0.07826	0.2273
34.7	20.26	33.19	2.037	3.61	0.06343	16.73	16.18	0.0791	0.2509
34.12	19.02	39.51	1.952	3.168	0.06152	14.29	14.15	0.07863	0.2987
wet enhanced									
34.48	25.12	20.14	1.281	3.967	0.1505	20.29	19.99	0.1319	0.1523
34.56	24.66	26.63	1.312	3.501	0.1503	19.87	19.43	0.1329	0.2013
34.78	24.78	29.79	1.447	3.515	0.15	20.59	19.94	0.1328	0.2252
34.82	24.66	32.89	1.607	3.536	0.1511	20.62	19.89	0.1326	0.2486
34.79	24.27	39.12	1.294	3.013	0.1521	20.5	19.55	0.1318	0.2957
34.57	26.54	20.2	1.735	4.581	0.2377	20.03	19.77	0.1802	0.1527
34.22	25.7	26.63	1.803	4.044	0.2347	17.27	17.2	0.1826	0.2013
34.53	25.71	29.78	1.775	3.887	0.2391	18.15	18.07	0.1822	0.2251
34.94	26.42	32.89	1.949	4.087	0.2575	22.64	21.85	0.1742	0.2486
34.54	25.48	39.15	1.841	3.652	0.2593	20.88	20.26	0.1751	0.2960
34.15	27.03	20.21	1.289	4.286	0.3232	20.32	20.24	0.2164	0.1528
34.18	26.74	26.67	0.9744	3.496	0.3276	20.97	20.79	0.217	0.2016
34.11	26.5	29.83	1.144	3.445	0.3289	20.58	20.41	0.2172	0.2255
33.97	26.22	32.94	1.162	3.288	0.3287	20.3	20.12	0.2171	0.2490
33.89	25.9	39.18	1.294	3.165	0.3298	20.05	19.86	0.2171	0.2962
34.65	21.76	20.35	2.027	4.271	0.0577	15.79	15.5	0.08015	0.1538
34.63	20.96	26.78	1.679	3.502	0.05767	15.34	15.12	0.0805	0.2025
34.77	20.66	29.98	1.588	3.253	0.05739	14.31	14.16	0.08075	0.2266
34.91	20.82	33.1	2.012	3.582	0.05867	15.99	15.51	0.07998	0.2502
34.79	20.16	39.4	1.995	3.344	0.05826	14.45	13.97	0.08055	0.2979

Appendix B. EES Code

```
"input Values"
"From Experiment"
DP_NOZZLE=0.198975          "Nozzle pressure difference in inH2O"
Tus_AIR=27.06791            "Temperature upstream of the heat exchanger in C"
Tds_AIR=23.6803          "Temperature downstream of the heat exchanger in C"
coolant=19.25892            "Coolant mass flow rate in lbm/min"
Tin_COOLANT=10.75617        "Coolant inlet temperaturc in C"
Tout_COOLANT=12.03968       "Coolant outlet temperaturc in C"
pt_test=0.219872            "Pressure drop through heat exchanger in inH2O"
T_dew_up =9.930495       "upstream dew point temperature in C"
T_dew_dn = 6.551329         "downstream dewpoint temperature in C"
T_infinity = 22          "ambient room temperature in C"
Patm=750.8                  "atmospheric pressure in mmHg"
noz_err=1                   “to add uncertainty associated with nozzle”
Nusselt_uncertainty=1       “to add uncertainty associated with correlation”

"Coolant Properties from curve fits"
mf=39                                   "mass % of Dowtherm 4000 in coolant mixture"
ml=mf/100
Tcool_K=converttemp(C,K,T_COOLANT)  "average coolant temp. in Kelvin"
rho_coola=exp(6.7491615501E+00+1.3834056594E-03*Tcool_K-2.8356666462E-
06*Tcool_K^2+5.1249487534E-03*mf-4.1953355636E-05*mf^2-3.6957657159E-
06*Tcool_K*mf+1.2232700342E-07*Tcool_K*mf^2)
rho_coolb=exp(-6.3573436849E-08*Tcool_K^2*mf+4.1466605761E-11*Tcool_K^2*mf^2-
5.6256865139E-15*Tcool_K^3*mf^3+1.2349378406E-10*Tcool_K^3*mf+4.4192089114E-
10*Tcool_K*mf^3)
rho_cool=rho_coola*rho_coolb                    "coolant density kg/m^3"
Kca=exp(-3.1348634984E+00+1.3814360766E-02*Tcool_K-1.7029980653E-05*Tcool_K^2-
5.7003610267E-02*mf+6.5326799517E-04*mf^2+6.0414689628E-04*Tcool_K*mf-6.4617945348E-
06*Tcool_K*mf^2)
Kcb=exp(-2.0666171150E-06*Tcool_K^2*mf+1.4032010938E-08*Tcool_K^2*mf^2-7.3924749685E-
14*Tcool_K^3*mf^3+1.9836620000E-09*Tcool_K^3*mf+7.1592190527E-09*Tcool_K*mf^3)
Kc=Kca*Kcb
CP_COOLANTa=exp(8.6425163658E-01+3.2983649059E-03*Tcool_K-4.8245491599E-
06*Tcool_K^2+4.1430129841E-02*mf-3.4915675121E-04*mf^2-4.1106062840E-
04*Tcool_K*mf+2.1047267827E-06*Tcool_K*mf^2)
CP_COOLANTb=exp(1.2154086417E-06*Tcool_K^2*mf-3.1673845039E-09*Tcool_K^2*mf^2-
9.9128411498E-16*Tcool_K^3*mf^3-1.1563635863E-09*Tcool_K^3*mf-6.7004804251E-
10*Tcool_K*mf^3)
CP_COOLANT=CP_COOLANTa*CP_COOLANTb      "coolant specific heat"
mu_coola=exp(1.5613560613E+01-1.1576320710E-01*Tcool_K+2.0794768121E-
04*Tcool_K^2+1.0691362447E+02*ml-5.1078070406E-01*ml^2-6.9464880099E-01*Tcool_K*ml-
5.6729890957E-01*Tcool_K*ml^2)
mu_coolb=exp(1.9829307580E-03*Tcool_K^2*ml+1.8661682823E-03*Tcool_K^2*ml^2-
2.5991503376E-06*Tcool_K^3*ml^3-2.7062727171E-06*Tcool_K^3*ml+2.4033982964E-
01*Tcool_K*ml^3)
mu_cool=mu_coola*mu_coolb
Pr=CP_COOLANT*mu_cool/Kc

"heat exchanger properties"
d_id_tube=.008              "inner diameter of tube m^2"
Aff=0.02783                 "minimum free flow area m^2"
Afr=0.044542             "frontal area m^2"
```

```
At=2.12769              "total heat transfer area m^2"
d_od_tube=0.01016               "outer tube diameter m^2"
Lc=.044                         "characteristic length, the depth of HEX, m"
Lt=3.7592               "length of tubing in HEX, m"
cf=1                    "cross flow correction factor"
A_ts=0.094479                   "tube side surface area"

"Air Side energy"
PT_NOZZLE=DP_NOZZLE*convert(InH2O, kPa)"Nozzle pressure drop in kPa
T_AIR=(Tus_AIR+Tds_AIR)/2 "Average air temp at heat exchanger"
CP_AIR_up=CP(AirH2O,T=Tus_AIR, P=P_noz_up-PT_NOZZLE, D=T_dew_up)
        "specific heat of air up stream"
CP_AIR_down=CP(AirH2O,T=Tds_AIR, P=P_noz_up-PT_NOZZLE-DELTA_P, D=T_dew_dn)
        "specific heat of air down stream"
CP_AIR=(CP_AIR_up+CP_AIR_down)/2                "specific heat average"
Q_AIR = (m_air*(h_air_up-h_air_dn)-m_water*h_water)*1000
        "sensible air side energy change in Watts"
h_air_up = Enthalpy(AirH2O, T=Tus_AIR, P=P_noz_up-PT_NOZZLE, D=T_dew_up)
        "upstream air/water enthalpy"
h_air_dn = Enthalpy(AirH2O, T=Tds_AIR, P=P_noz_up-PT_NOZZLE-DELTA_P, D=T_dew_dn)
        "downstream air/water enthalpy"

"air mass flow calculation"
m_air = epsilon*C*.25*pi*Di^2*sqrt(2*PT_NOZZLE*1000*rho_air_noz_up/(1-beta^4))          "air
mass flow rate from nozzle calculations"
kappa = CP(Air, T=Tus_AIR)/CV(Air, T=Tus_AIR)       "Specific heat ratio"
tau = 1 - PT_NOZZLE/P_noz_up
epsilon = sqrt((kappa/(kappa-1)*tau^(2/kappa)) * ((1-beta^4)/(1-beta^4*tau^(2/kappa)))* ((1-tau^(1-
1/kappa))/(1-tau)))
Do = 14*.0254           " m "
Di = 6*.0254            " m "
beta = Di/Do
Ra_D = m_air/(.25*pi*mu_air_noz_up*Do)
rho_air_noz_up = Density(AirH2O, T=Tus_AIR, P=P_noz_up, D=T_dew_up)
mu_air_noz_up = Viscosity(AirH2O, T=Tus_AIR, P=P_noz_up, D=T_dew_up)
mu_air_noz_down = Viscosity(AirH2O, T=Tds_AIR, P=P_noz_up-PT_NOZZLE-DELTA_P,
D=T_dew_dn)
mu_air=(mu_air_noz_up+mu_air_noz_down)/2
        C = (.9975 - .00653*sqrt(1e6*beta/Ra_D))*noz_err
P_infinity = Patm*convert(mmHg, kPa)*CT*CG
                        " Pa, absolute ambient pressure"
        CT = (1+1.84e-4*T_infinity)/(1+1.818e-4*T_infinity)
                        " Temperature correction factor "
        CG = (980.616/980.665)*(1-.0026373*cos(2*phi)+5.9e-6*cos(2*phi)^2)
        " Gravitation correction factor "
phi = 40                        "deg, latitude"
P_noz_up = (0.057-(-.009))*2*convert(inH2O, kPa) + P_infinity
        " Pa, absolute nozzle up pressure"

"energy of condensed vapor"
water_up=HUMRAT(AirH2O,T=Tus_AIR,P=P_noz_up-PT_NOZZLE,D=T_dew_up)
        "humidity ratio of upstream air"
water_down=HUMRAT(AirH2O,T=Tds_AIR,P=P_noz_up-PT_NOZZLE-DELTA_P, D=T_dew_dn)
        "humidity ratio of downstream air"
“water_down=water_up”                   "use for dry tests"
mw_up=water_up/(1+water_up)             "convert humidity ratio to mass fraction"
```

```
mw_down=water_down/(1+water_down)          "convert humidity ratio to mass fraction"
m_water=m_air*(mw_up-mw_down)    "mass flow rate of condensing water on heat exchanger"
h_water=ENTHALPY(Steam,T=(T_dew_up+T_dew_dn)/2,P=P_noz_up-PT_NOZZLE)

"coolant side energy"
M_COOLANT=coolant*convert(lbm/min,kg/s)   "coolant mass flow rate in kg/s"
T_COOLANT=(Tin_COOLANT+Tout_COOLANT)/2
                                  "Average coolant temperature in HEX"
Q_COOLANT=M_COOLANT*CP_COOLANT*(Tout_COOLANT-Tin_COOLANT)*1000
        "coolant side energy change in Watts"

"energy balance"
Qavg=(Q_COOLANT+Q_AIR)/2                   "Average energy change"
ENERGYBALANCE=(Q_AIR-Qavg)/Qavg*100 "percent error in energy balance"

"air side calculations"
D_H=4*Aff*Lc/At                  "hydraulic diameter of heat exchanger"
G=M_AIR/Aff                      "maximum mass velocity "
RE_DH=G*D_H/mu_air          "air side Reynolds number based on hydraulic diameter"
rho_in=DENSITY(AirH2O,T=Tus_AIR,P=P_noz_up-PT_NOZZLE,D=T_dew_up)
        "density of air upstream"
rho_out=DENSITY(AirH2O,T=Tds_AIR,P=P_noz_up-PT_NOZZLE-DELTA_P, D=T_dew_dn)
        "density of air downstream"
rho_ave=(rho_in+rho_out)/2    "average density"

"tube side calculations"
T_mean_tube=(T_AIR+T_COOLANT)/2                    "mean temperature of tube in C"
kt=k_('Copper', T_mean_tube)"W/m*K     thermal conductivity of copper tube"
mu_coolant=mu_cool*convert(milliPa*s,kg/(s*m)) "viscosity coolant from dowther"

f_INSIDE=(0.79*LN(RE_D)-1.64)^(-2)  "Tube side friction factor, Petukhov "
RE_D=4*M_COOLANT/(pi*d_id_tube*mu_coolant)
                  "tube-side reynolds number based on tube diameter"
NUSSELT_D=((f_INSIDE/8)*(RE_D-1000)*Pr)/(1.07+12.7*(f_INSIDE/8)^(1/2)*(Pr^(2/3)-
1))*Nusselt_uncertainty                  "tube side Nusselt number from Gneilinski correlation"
h_ts=NUSSELT_D*Kc/d_id_tube                  "tube-side convective heat transfer coefficient from
definition of Nusselt Number"
eta_o*h_air=(At*(cf*LMTD/Qavg-LN(d_od_tube/d_id_tube)/(2*pi*Kt*Lt)-1/(h_ts*A_ts)))^(-1)        "the
product of overall surface efficiency eta_o and overall convective heat transfer coefficient ho"
eta_o=1-(At-A_ts)/At*(1-eta_FIN)
LMTD=((Tus_AIR-Tout_COOLANT)-(Tds_AIR-Tin_COOLANT))/LN((Tus_AIR-
Tout_COOLANT)/(Tds_AIR-Tin_COOLANT))"Log mean temperature difference"
U=Qavg/(LMTD*At)                                    "Overall heat transfer coefficient"

"friction coefficient calculation"
DELTA_P=pt_test*convert(inH2O,kPa)          "pressure drop across HEX in kPa"

DELTA_P*1000=(G)^2/(2*rho_in)*((1+(Aff/Afr)^2)*(rho_in/rho_out-1)+f*At/Aff*rho_in/rho_ave)
                        "friction factor calculation"
k=CONDUCTIVITY(AirH2O,T=T_AIR,P=P_noz_up-PT_NOZZLE-
DELTA_P/2,D=(T_dew_up+T_dew_dn)/2)                "thermal conductivity of air at average temp,
average pressure, and average dew point"
V=m_air/(Density(AirH2O, T=Tus_AIR, P=P_noz_up, D=T_dew_up)*(Aff))
        "m/s  Average velocity in heat exchanger"
J_H=h_air/(rho_ave*V*CP_AIR*1000)*(1000*CP_AIR*mu_air/k)^(2/3)
        "colburn j factor"
```

```
"modified volume goodness calculation"
nhb=eta_o*h_air*beta_1        "heat transfer rate per unit core volume per unit temperatue difference"
beta_1=At/(Afr*Lc)            "heat transfer surface area per unit core volume"
E=pt_test*convert(inH2O,Pa)/At        "air side Pressure drop per unit surface area"
Eb=E*beta_1*m_air/rho_air_noz_up    "Pressure drop per unit core volume"

"Uncertainty Analysis"

"Sector method for calculation of fin efficiency for plain fin Samsung compact heat exchanger"

Ft=.005*convert(in,m)                    "fin thickness, m"
ka=k_('Aluminum', T_mean_tube)                "fin conductivity"
m=SQRT(2*h_air/(ka*Ft))
ri=.00508                                "fin inner diameter , m"

"For an interior fin"
"only need to do the first four sectors due to symmetry"
"Zone 1    constant L edge"
            M1=.0125                     "transverse tube spacing"
            L1=.012
            Nt=4                         "total number of sectors in this zone"
      "sector a"
            eta_1a=2*ri/(m*(roa^2-ri^2))*(B1a)  "sector efficiency"
            B1a=(Bessel_K1(m*ri)*Bessel_I1(m*roa)-
Bessel_K1(m*roa)*Bessel_I1(m*ri))/(Bessel_K1(m*roa)*Bessel_I0(m*ri)+Bessel_K0(m*ri)*Bessel_I1(m
*roa))
            na=1                                 "first sector in this zone"
            Ra=M1/ri*SQRT(((2*na-1)/(2*Nt))^2*(L1/M1)^2+1)
            S1a=(ri^2/2)*(Ra^2-1)*(ARCTAN(na*L1/(Nt*M1))-ARCTAN((na-1)*L1/(Nt*M1)))  "Surface
area of this sector"
            roa=ri*Ra
      "sector b"
            eta_1b=2*ri/(m*(rob^2-ri^2))*(B1b)  "sector efficiency"
            B1b=(Bessel_K1(m*ri)*Bessel_I1(m*rob)-
Bessel_K1(m*rob)*Bessel_I1(m*ri))/(Bessel_K1(m*rob)*Bessel_I0(m*ri)+Bessel_K0(m*ri)*Bessel_I1(m
*rob))
            nb=2                                 "second sector in this zone"
            Rb=M1/ri*SQRT(((2*nb-1)/(2*Nt))^2*(L1/M1)^2+1)
            S1b=(ri^2/2)*(Rb^2-1)*(ARCTAN(nb*L1/(Nt*M1))-ARCTAN((nb-1)*L1/(Nt*M1)))  "Surface
area of this sector"
            rob=ri*Rb
      "sector c"
            eta_1c=2*ri/(m*(roc^2-ri^2))*(B1c)  "sector efficiency"
            B1c=(Bessel_K1(m*ri)*Bessel_I1(m*roc)-
Bessel_K1(m*roc)*Bessel_I1(m*ri))/(Bessel_K1(m*roc)*Bessel_I0(m*ri)+Bessel_K0(m*ri)*Bessel_I1(m*
roc))
            nc=3                                 "third sector in this zone"
            Rc=M1/ri*SQRT(((2*nc-1)/(2*Nt))^2*(L1/M1)^2+1)
            S1c=(ri^2/2)*(Rc^2-1)*(ARCTAN(nc*L1/(Nt*M1))-ARCTAN((nc-1)*L1/(Nt*M1)))  "Surface
area of this sector"
            roc=ri*Rc
      "sector d"
            eta_1d=2*ri/(m*(rod^2-ri^2))*(B1d)  "sector efficiency"
```

```
        B1d=(Bessel_K1(m*ri)*Bessel_I1(m*rod)-
Bessel_K1(m*rod)*Bessel_I1(m*ri))/(Bessel_K1(m*rod)*Bessel_I0(m*ri)+Bessel_K0(m*ri)*Bessel_I1(m
*rod))
        nd=4                                    "fourth sector in this zone"
        Rd=M1/ri*SQRT(((2*nd-1)/(2*Nt))^2*(L1/M1)^2+1)
        S1d=(ri^2/2)*(Rd^2-1)*(ARCTAN(nd*L1/(Nt*M1))-ARCTAN((nd-1)*L1/(Nt*M1)))  "Surface
area of this sector"
        rod=ri*Rd

"Zone 2    constant M edge"
        M2=M1
        L2=L1
    "sector a"
        eta_2a=2*ri/(m*(ro2a^2-ri^2))*(B2a)  "sector efficiency"
        B2a=(Bessel_K1(m*ri)*Bessel_I1(m*ro2a)-
Bessel_K1(m*ro2a)*Bessel_I1(m*ri))/(Bessel_K1(m*ro2a)*Bessel_I0(m*ri)+Bessel_K0(m*ri)*Bessel_I1(
m*ro2a))
        R2a=M2/ri*SQRT(((2*na-1)/(2*Nt))^2+(L2/M2)^2)
        S2a=(ri^2/2)*(R2a^2-1)*(ARCTAN(na*M2/(Nt*L2))-ARCTAN((na-1)*M2/(Nt*L2)))
"Surface area of this sector"
        ro2a=ri*R2a
    "sector b"
        eta_2b=2*ri/(m*(ro2b^2-ri^2))*(B2b)  "sector efficiency"
        B2b=(Bessel_K1(m*ri)*Bessel_I1(m*ro2b)-
Bessel_K1(m*ro2b)*Bessel_I1(m*ri))/(Bessel_K1(m*ro2b)*Bessel_I0(m*ri)+Bessel_K0(m*ri)*Bessel_I1(
m*ro2b))
        R2b=M2/ri*SQRT(((2*nb-1)/(2*Nt))^2+(L2/M2)^2)
        S2b=(ri^2/2)*(R2b^2-1)*(ARCTAN(nb*M2/(Nt*L2))-ARCTAN((nb-1)*M2/(Nt*L2)))
"Surface area of this sector"
        ro2b=ri*R2b
    "sector c"
        eta_2c=2*ri/(m*(ro2c^2-ri^2))*(B2c)  "sector efficiency"
        B2c=(Bessel_K1(m*ri)*Bessel_I1(m*ro2c)-
Bessel_K1(m*ro2c)*Bessel_I1(m*ri))/(Bessel_K1(m*ro2c)*Bessel_I0(m*ri)+Bessel_K0(m*ri)*Bessel_I1(
m*ro2c))
        R2c=M2/ri*SQRT(((2*nc-1)/(2*Nt))^2+(L2/M2)^2)
        S2c=(ri^2/2)*(R2c^2-1)*(ARCTAN(nc*M2/(Nt*L2))-ARCTAN((nc-1)*M2/(Nt*L2)))
"Surface area of this sector"
        ro2c=ri*R2c
    "sector d"
        eta_2d=2*ri/(m*(ro2d^2-ri^2))*(B2d)  "sector efficiency"
        B2d=(Bessel_K1(m*ri)*Bessel_I1(m*ro2d)-
Bessel_K1(m*ro2d)*Bessel_I1(m*ri))/(Bessel_K1(m*ro2d)*Bessel_I0(m*ri)+Bessel_K0(m*ri)*Bessel_I1(
m*ro2d))
        R2d=M2/ri*SQRT(((2*nd-1)/(2*Nt))^2+(L2/M2)^2)
        S2d=(ri^2/2)*(R2d^2-1)*(ARCTAN(nd*M2/(Nt*L2))-ARCTAN((nd-1)*M2/(Nt*L2)))
"Surface area of this sector"
        ro2d=ri*R2d

"Zone 3"
    "sector a"
        ro3a=.01259  "calculated by hand"
        eta_3a=2*ri/(m*(ro3a^2-ri^2))*(B3a)  "sector efficiency"
        B3a=(Bessel_K1(m*ri)*Bessel_I1(m*ro3a)-
Bessel_K1(m*ro3a)*Bessel_I1(m*ri))/(Bessel_K1(m*ro3a)*Bessel_I0(m*ri)+Bessel_K0(m*ri)*Bessel_I1(
m*ro3a))
```

```
                S3a=.000013305  "Surface area of this sector , calculated by hand"
        "sector b"
                ro3b=.012873 "calculated by hand"
                eta_3b=2*ri/(m*(ro3b^2-ri^2))*(B3b)  "sector efficiency"
                B3b=(Bessel_K1(m*ri)*Bessel_I1(m*ro3b)-
Bessel_K1(m*ro3b)*Bessel_I1(m*ri))/(Bessel_K1(m*ro3b)*Bessel_I0(m*ri)+Bessel_K0(m*ri)*Bessel_I1(
m*ro3b))
                S3b=.0000141"Surface area of this sector , calculated by hand"
        "sector c"
                ro3c=.013396  "calculated by hand"
                eta_3c=2*ri/(m*(ro3c^2-ri^2))*(B3c)  "sector efficiency"
                B3c=(Bessel_K1(m*ri)*Bessel_I1(m*ro3c)-
Bessel_K1(m*ro3c)*Bessel_I1(m*ri))/(Bessel_K1(m*ro3c)*Bessel_I0(m*ri)+Bessel_K0(m*ri)*Bessel_I1(
m*ro3c))
                S3c=.000015891 "Surface area of this sector , calculated by hand"
        "sector d"
                ro3d=.014254  "calculated by hand"
                eta_3d=2*ri/(m*(ro3d^2-ri^2))*(B3d)  "sector efficiency"
                B3d=(Bessel_K1(m*ri)*Bessel_I1(m*ro3d)-
Bessel_K1(m*ro3d)*Bessel_I1(m*ri))/(Bessel_K1(m*ro3d)*Bessel_I0(m*ri)+Bessel_K0(m*ri)*Bessel_I1(
m*ro3d))
                S3d=.0000192038  "Surface area of this sector , calculated by hand"

"zone 4"
        "sector a"
                ro4a=.010128 "calculated by hand"
                eta_4a=2*ri/(m*(ro4a^2-ri^2))*(B4a)  "sector efficiency"
                B4a=(Bessel_K1(m*ri)*Bessel_I1(m*ro4a)-
Bessel_K1(m*ro4a)*Bessel_I1(m*ri))/(Bessel_K1(m*ro4a)*Bessel_I0(m*ri)+Bessel_K0(m*ri)*Bessel_I1(
m*ro4a))
                S4a=.000011392  "Surface area of this sector , calculated by hand"
        "sector b"
                ro4b=.010548 "calculated by hand"
                eta_4b=2*ri/(m*(ro4b^2-ri^2))*(B4b)  "sector efficiency"
                B4b=(Bessel_K1(m*ri)*Bessel_I1(m*ro4b)-
Bessel_K1(m*ro4b)*Bessel_I1(m*ri))/(Bessel_K1(m*ro4b)*Bessel_I0(m*ri)+Bessel_K0(m*ri)*Bessel_I1(
m*ro4b))
                S4b=.000012639  "Surface area of this sector , calculated by hand"
        "sector c"
                ro4c=.011389 "calculated by hand"
                eta_4c=2*ri/(m*(ro4c^2-ri^2))*(B4c)  "sector efficiency"
                B4c=(Bessel_K1(m*ri)*Bessel_I1(m*ro4c)-
Bessel_K1(m*ro4c)*Bessel_I1(m*ri))/(Bessel_K1(m*ro4c)*Bessel_I0(m*ri)+Bessel_K0(m*ri)*Bessel_I1(
m*ro4c))
                S4c=.000015748  "Surface area of this sector , calculated by hand"
        "sector d"
                ro4d=.013004 "calculated by hand"
                eta_4d=2*ri/(m*(ro4d^2-ri^2))*(B4d)  "sector efficiency"
                B4d=(Bessel_K1(m*ri)*Bessel_I1(m*ro4d)-
Bessel_K1(m*ro4d)*Bessel_I1(m*ri))/(Bessel_K1(m*ro4d)*Bessel_I0(m*ri)+Bessel_K0(m*ri)*Bessel_I1(
m*ro4d))
                S4d=.0000227208  "Surface area of this sector , calculated by hand"

"Calculation of average eta for this tube"
```

```
num=(eta_1a*S1a+eta_1b*S1b+eta_1c*S1c+eta_1d*S1d+eta_2a*S2a+eta_2b*S2b+eta_2c*S2c+eta_
2d*S2d+eta_3a*S3a+eta_3b*S3b+eta_3c*S3c+eta_3d*S3d+eta_4a*S4a+eta_4b*S4b+eta_4c*S4c+et
a_4d*S4d)
den=(S1a+S1b+S1c+S1d+S2a+S2b+S2c+S2d+S3a+S3b+S3c+S3d+S4a+S4b+S4c+S4d)
eta_i=num/den

"Type L tube, zone 1,2,3,4 ,& 8 are the same as previous"
"Zone 5"
	"sector a"
		ro5a=.010186 "calculated by hand"
		eta_5a=2*ri/(m*(ro5a^2-ri^2))*(B5a)  "sector efficiency"
		B5a=(Bessel_K1(m*ri)*Bessel_I1(m*ro5a)-
Bessel_K1(m*ro5a)*Bessel_I1(m*ri))/(Bessel_K1(m*ro5a)*Bessel_I0(m*ri)+Bessel_K0(m*ri)*Bessel_I1(
m*ro5a))
		S5a=.000013775 "Surface area of this sector , calculated by hand"
	"sector b"
		ro5b=.011008 "calculated by hand"
		eta_5b=2*ri/(m*(ro5b^2-ri^2))*(B5b)  "sector efficiency"
		B5b=(Bessel_K1(m*ri)*Bessel_I1(m*ro5b)-
Bessel_K1(m*ro5b)*Bessel_I1(m*ri))/(Bessel_K1(m*ro5b)*Bessel_I0(m*ri)+Bessel_K0(m*ri)*Bessel_I1(
m*ro5b))
		S5b=.000016035 "Surface area of this sector , calculated by hand"
	"sector c"
		ro5c=.013046 "calculated by hand"
		eta_5c=2*ri/(m*(ro5c^2-ri^2))*(B5c)  "sector efficiency"
		B5c=(Bessel_K1(m*ri)*Bessel_I1(m*ro5c)-
Bessel_K1(m*ro5c)*Bessel_I1(m*ri))/(Bessel_K1(m*ro5c)*Bessel_I0(m*ri)+Bessel_K0(m*ri)*Bessel_I1(
m*ro5c))
		S5c=.00002234"Surface area of this sector , calculated by hand"
	"sector d"
		ro5d=.017739 "calculated by hand"
		eta_5d=2*ri/(m*(ro5d^2-ri^2))*(B5d)  "sector efficiency"
		B5d=(Bessel_K1(m*ri)*Bessel_I1(m*ro5d)-
Bessel_K1(m*ro5d)*Bessel_I1(m*ri))/(Bessel_K1(m*ro5d)*Bessel_I0(m*ri)+Bessel_K0(m*ri)*Bessel_I1(
m*ro5d))
		S5d=.00004035  "Surface area of this sector , calculated by hand"

"Zone 6"
	"sector a"
		ro6a=.018572 "calculated by hand"
		eta_6a=2*ri/(m*(ro6a^2-ri^2))*(B6a)  "sector efficiency"
		B6a=(Bessel_K1(m*ri)*Bessel_I1(m*ro6a)-
Bessel_K1(m*ro6a)*Bessel_I1(m*ri))/(Bessel_K1(m*ro6a)*Bessel_I0(m*ri)+Bessel_K0(m*ri)*Bessel_I1(
m*ro6a))
		S6a=.000021312 "Surface area of this sector , calculated by hand"
	"sector b"
		ro6b=.018863 "calculated by hand"
		eta_6b=2*ri/(m*(ro6b^2-ri^2))*(B6b)  "sector efficiency"
		B6b=(Bessel_K1(m*ri)*Bessel_I1(m*ro6b)-
Bessel_K1(m*ro6b)*Bessel_I1(m*ri))/(Bessel_K1(m*ro6b)*Bessel_I0(m*ri)+Bessel_K0(m*ri)*Bessel_I1(
m*ro6b))
		S6b=.000021978 "Surface area of this sector , calculated by hand"
	"sector c"
		ro6c=.01947 "calculated by hand"
		eta_6c=2*ri/(m*(ro6c^2-ri^2))*(B6c)  "sector efficiency"
```

```
		B6c=(Bessel_K1(m*ri)*Bessel_I1(m*ro6c)-
Bessel_K1(m*ro6c)*Bessel_I1(m*ri))/(Bessel_K1(m*ro6c)*Bessel_I0(m*ri)+Bessel_K0(m*ri)*Bessel_I1(
m*ro6c))
		S6c=.000023412"Surface area of this sector , calculated by hand"
	"sector d"
		ro6d=.020443 "calculated by hand"
		eta_6d=2*ri/(m*(ro6d^2-ri^2))*(B6d)  "sector efficiency"
		B6d=(Bessel_K1(m*ri)*Bessel_I1(m*ro6d)-
Bessel_K1(m*ro6d)*Bessel_I1(m*ri))/(Bessel_K1(m*ro6d)*Bessel_I0(m*ri)+Bessel_K0(m*ri)*Bessel_I1(
m*ro6d))
		S6d=.000025798  "Surface area of this sector , calculated by hand"

"Zone 7"
	"sector a"
		ro7a=.018643 "calculated by hand"
		eta_7a=2*ri/(m*(ro7a^2-ri^2))*(B7a)  "sector efficiency"
		B7a=(Bessel_K1(m*ri)*Bessel_I1(m*ro7a)-
Bessel_K1(m*ro7a)*Bessel_I1(m*ri))/(Bessel_K1(m*ro7a)*Bessel_I0(m*ri)+Bessel_K0(m*ri)*Bessel_I1(
m*ro7a))
		S7a=.000030201 "Surface area of this sector , calculated by hand"
	"sector b"
		ro7b=.019225 "calculated by hand"
		eta_7b=2*ri/(m*(ro7b^2-ri^2))*(B7b)  "sector efficiency"
		B7b=(Bessel_K1(m*ri)*Bessel_I1(m*ro7b)-
Bessel_K1(m*ro7b)*Bessel_I1(m*ri))/(Bessel_K1(m*ro7b)*Bessel_I0(m*ri)+Bessel_K0(m*ri)*Bessel_I1(
m*ro7b))
		S7b=.00003213 "Surface area of this sector , calculated by hand"
	"sector c"
		ro7c=.020528 "calculated by hand"
		eta_7c=2*ri/(m*(ro7c^2-ri^2))*(B7c)  "sector efficiency"
		B7c=(Bessel_K1(m*ri)*Bessel_I1(m*ro7c)-
Bessel_K1(m*ro7c)*Bessel_I1(m*ri))/(Bessel_K1(m*ro7c)*Bessel_I0(m*ri)+Bessel_K0(m*ri)*Bessel_I1(
m*ro7c))
		S7c=.000036556"Surface area of this sector , calculated by hand"
	"sector d"
		ro7d=.018846 "calculated by hand"
		eta_7d=2*ri/(m*(ro7d^2-ri^2))*(B7d)  "sector efficiency"
		B7d=(Bessel_K1(m*ri)*Bessel_I1(m*ro7d)-
Bessel_K1(m*ro7d)*Bessel_I1(m*ri))/(Bessel_K1(m*ro7d)*Bessel_I0(m*ri)+Bessel_K0(m*ri)*Bessel_I1(
m*ro7d))
		S7d=.0000315  "Surface area of this sector , calculated by hand"

"Type L eta calculation"

	 "1 is same as 8"
num_L=num+eta_5a*S5a+eta_5b*S5b+eta_5c*S5c+eta_5d*S5d+eta_6a*S6a+eta_6b*S6b+eta_6c*S6
c+eta_6d*S6d+eta_7a*S7a+eta_7b*S7b+eta_7c*S7c+eta_7d*S7d+eta_1a*S1a+eta_1b*S1b+eta_1c*
S1c+eta_1d*S1d
den_L=den+S5a+S5b+S5c+S5d+S6a+S6b+S6c+S6d+S7a+S7b+S7c+S7d+S1a+S1b+S1c+S1d
eta_L=num_L/den_L



"Type K tube, zone1,2,3,4 are the same as previous"
"Zone 9"
	"sector a"
```

```
                ro9a=.010046 "calculated by hand"
                eta_9a=2*ri/(m*(ro9a^2-ri^2))*(B9a)  "sector efficiency"
                B9a=(Bessel_K1(m*ri)*Bessel_I1(m*ro9a)-
Bessel_K1(m*ro9a)*Bessel_I1(m*ri))/(Bessel_K1(m*ro9a)*Bessel_I0(m*ri)+Bessel_K0(m*ri)*Bessel_I1(
m*ro9a))
                S9a=.00000679665 "Surface area of this sector , calculated by hand"
        "sector b"
                ro9b=.010235 "calculated by hand"
                eta_9b=2*ri/(m*(ro9b^2-ri^2))*(B9b)  "sector efficiency"
                B9b=(Bessel_K1(m*ri)*Bessel_I1(m*ro9b)-
Bessel_K1(m*ro9b)*Bessel_I1(m*ri))/(Bessel_K1(m*ro9b)*Bessel_I0(m*ri)+Bessel_K0(m*ri)*Bessel_I1(
m*ro9b))
                S9b=.00000705255 "Surface area of this sector , calculated by hand"
        "sector c"
                ro9c=.01063 "calculated by hand"
                eta_9c=2*ri/(m*(ro9c^2-ri^2))*(B9c)  "sector efficiency"
                B9c=(Bessel_K1(m*ri)*Bessel_I1(m*ro9c)-
Bessel_K1(m*ro9c)*Bessel_I1(m*ri))/(Bessel_K1(m*ro9c)*Bessel_I0(m*ri)+Bessel_K0(m*ri)*Bessel_I1(
m*ro9c))
                S9c=.0000076044"Surface area of this sector , calculated by hand"
        "sector d"
                ro9d=.011272 "calculated by hand"
                eta_9d=2*ri/(m*(ro9d^2-ri^2))*(B9d)  "sector efficiency"
                B9d=(Bessel_K1(m*ri)*Bessel_I1(m*ro9d)-
Bessel_K1(m*ro9d)*Bessel_I1(m*ri))/(Bessel_K1(m*ro9d)*Bessel_I0(m*ri)+Bessel_K0(m*ri)*Bessel_I1(
m*ro9d))
                S9d=.0000085464  "Surface area of this sector , calculated by hand"

"Zone 10"
        "sector a"
                ro10a=.006103 "calculated by hand"
                eta_10a=2*ri/(m*(ro10a^2-ri^2))*(B10a)  "sector efficiency"
                B10a=(Bessel_K1(m*ri)*Bessel_I1(m*ro10a)-
Bessel_K1(m*ro10a)*Bessel_I1(m*ri))/(Bessel_K1(m*ro10a)*Bessel_I0(m*ri)+Bessel_K0(m*ri)*Bessel_
I1(m*ro10a))
                S10a=.000004742 "Surface area of this sector , calculated by hand"
        "sector b"
                ro10b=.00655"calculated by hand"
                eta_10b=2*ri/(m*(ro10b^2-ri^2))*(B10b)  "sector efficiency"
                B10b=(Bessel_K1(m*ri)*Bessel_I1(m*ro10b)-
Bessel_K1(m*ro10b)*Bessel_I1(m*ri))/(Bessel_K1(m*ro10b)*Bessel_I0(m*ri)+Bessel_K0(m*ri)*Bessel_
I1(m*ro10b))
                S10b=.000005449 "Surface area of this sector , calculated by hand"
        "sector c"
                ro10c=.007638 "calculated by hand"
                eta_10c=2*ri/(m*(ro10c^2-ri^2))*(B10c)  "sector efficiency"
                B10c=(Bessel_K1(m*ri)*Bessel_I1(m*ro10c)-
Bessel_K1(m*ro10c)*Bessel_I1(m*ri))/(Bessel_K1(m*ro10c)*Bessel_I0(m*ri)+Bessel_K0(m*ri)*Bessel_
I1(m*ro10c))
                S10c=.00000736"Surface area of this sector , calculated by hand"
        "sector d"
                ro10d=.010021"calculated by hand"
                eta_10d=2*ri/(m*(ro10d^2-ri^2))*(B10d)  "sector efficiency"
                B10d=(Bessel_K1(m*ri)*Bessel_I1(m*ro10d)-
Bessel_K1(m*ro10d)*Bessel_I1(m*ri))/(Bessel_K1(m*ro10d)*Bessel_I0(m*ri)+Bessel_K0(m*ri)*Bessel_
I1(m*ro10d))
```

```
        S10d=.000012448 "Surface area of this sector , calculated by hand"

"zone 11 is equal to zone 10 by symmetry"

"Zone 12"
    "sector a"
        ro12a=.013574 "calculated by hand"
        eta_12a=2*ri/(m*(ro12a^2-ri^2))*(B12a)  "sector efficiency"
        B12a=(Bessel_K1(m*ri)*Bessel_I1(m*ro12a)-
Bessel_K1(m*ro12a)*Bessel_I1(m*ri))/(Bessel_K1(m*ro12a)*Bessel_I0(m*ri)+Bessel_K0(m*ri)*Bessel_
I1(m*ro12a))
        S12a=.0000135 "Surface area of this sector , calculated by hand"
    "sector b"
        ro12b=.013864"calculated by hand"
        eta_12b=2*ri/(m*(ro12b^2-ri^2))*(B12b)  "sector efficiency"
        B12b=(Bessel_K1(m*ri)*Bessel_I1(m*ro12b)-
Bessel_K1(m*ro12b)*Bessel_I1(m*ri))/(Bessel_K1(m*ro12b)*Bessel_I0(m*ri)+Bessel_K0(m*ri)*Bessel_
I1(m*ro12b))
        S12b=.0000135 "Surface area of this sector , calculated by hand"
    "sector c"
        ro12c=.014427 "calculated by hand"
        eta_12c=2*ri/(m*(ro12c^2-ri^2))*(B12c)  "sector efficiency"
        B12c=(Bessel_K1(m*ri)*Bessel_I1(m*ro12c)-
Bessel_K1(m*ro12c)*Bessel_I1(m*ri))/(Bessel_K1(m*ro12c)*Bessel_I0(m*ri)+Bessel_K0(m*ri)*Bessel_
I1(m*ro12c))
        S12c=.0000135"Surface area of this sector , calculated by hand"
    "sector d"
        ro12d=.013218"calculated by hand"
        eta_12d=2*ri/(m*(ro12d^2-ri^2))*(B12d)  "sector efficiency"
        B12d=(Bessel_K1(m*ri)*Bessel_I1(m*ro12d)-
Bessel_K1(m*ro12d)*Bessel_I1(m*ri))/(Bessel_K1(m*ro12d)*Bessel_I0(m*ri)+Bessel_K0(m*ri)*Bessel_
I1(m*ro12d))
        S12d=.0000105 "Surface area of this sector, calculated by hand"

"Type K eta calculation"


num_K=num+eta_9a*S9a+eta_9b*S9b+eta_9c*S9c+eta_9d*S9d+eta_10a*S10a+eta_10b*S10b+eta_
10c*S10c+eta_10d*S10d+eta_10a*S10a+eta_10b*S10b+eta_10c*S10c+eta_10d*S10d+eta_12a*S12
a+eta_12b*S12b+eta_12c*S12c+eta_12d*S12d
den_K=den+S9a+S9b+S9c+S9d+S10a+S10b+S10c+S10d+S10a+S10b+S10c+S10d+S12a+S12b+S1
2c+S12d
eta_K=num_K/den_K

"Total fin efficiency"
eta_FIN=(eta_i*den*12+eta_K*den_K*2+eta_L*den_L*2)/(den*12+den_K*2+den_L*2)
```